# Evasion Under Blockchain Sanctions

Endong Liu
University of Birmingham
Birmingham, United Kingdom

Mark Ryan
University of Birmingham
Birmingham, United Kingdom

Liyi Zhou*
The University of Sydney
Sydney, Australia

Pascal Berrang*
University of Birmingham
Birmingham, United Kingdom

## ABSTRACT

Sanctioning blockchain addresses has become a common regulatory response to malicious activities. However, enforcement on permissionless blockchains remains challenging due to complex transaction flows and sophisticated fund-obfuscation techniques. Using cryptocurrency mixing tool Tornado Cash as a case study, we quantitatively assess the effectiveness of U.S. Office of Foreign Assets Control (OFAC) sanctions over a 957-day period, covering 6.79 million Ethereum blocks and 1.07 billion transactions. Our analysis reveals that while OFAC sanctions reduced overall Tornado Cash deposit volume by 71.03% to approximately 2 billion USD, attackers still relied on Tornado Cash in 78.33% of Ethereum-related security incidents, underscoring persistent evasion strategies.

We identify three structural limitations in current sanction enforcement practices: *(i)* the susceptibility of binary sanction classifications to dusting attacks; *(ii)* fragmented censorship by blockchain producers; and *(iii)* the complexity of obfuscation services exploited by users. To address these gaps, we introduce a more practical algorithm for scoring and tracking, grounded in quantitative impurity. On average, our algorithm processes Ethereum blocks within $0.07 \pm 0.03$ seconds and achieves 97.61% precision and 74.08% recall when evaluated on the Bybit exploit. Our findings contribute to ongoing discussions around regulatory effectiveness in Decentralized Finance by providing empirical evidence, clarifying enforcement challenges, and informing future compliance strategies in response to sanctions and blockchain-based security risks.

## KEYWORDS

Blockchain sanctions, Tornado Cash, ByBit, OFAC, fund obfuscation, transaction tracking, compliance, Decentralized Finance, DeFi

## 1 INTRODUCTION

Sanctioning or blacklisting blockchain addresses is a strategy used by regulators to counter activities such as money laundering and terrorist financing. Despite ongoing efforts, enforcing sanctions on permissionless blockchains remains challenging, due to the complexity of transaction flows and the ease with which assets can be moved across addresses and protocols. For example, the U.S. Office of Foreign Assets Control (OFAC) sanctioned 170 addresses on Ethereum [7] that collectively held an initial balance of 499, 769.74 ETH (983 million USD) at the time of designation. Following these sanctions, adversaries transferred funds to newly created addresses and employed a range of obfuscation techniques to evade detection. By the end of the observation period (March 21, 2025), only 145, 579.38 ETH (286 million USD) remained.

Among these OFAC-sanctioned addresses, Tornado Cash (TC) represents the most significant case, constituting 44.17% of the initial and 99.12% of the remaining balance. As a privacy-focused cryptocurrency mixing pool, TC can break the on-chain linkability between deposit and withdrawal transactions. From our empirical analysis, TC processed over 2 billion USD during the sanctioned period from August 8, 2022 [38] to March 21, 2025 [39] (957 days). Remarkably, in 78.33% of 60 Ethereum-related security incidents during this period, attackers continued to leverage TC, illustrating persistent circumvention of sanctions by sophisticated actors. While prior research has predominantly focused on tracing security incidents [17, 21, 41, 46, 49] or reconstructing the linkability of anonymous transactions [11, 19, 42, 43], our study broadly assesses regulatory effectiveness by systematically evaluating the impact of sanctions. We identify three structural limitations in the current sanction enforcement framework:

(1) **Binary Classification Vulnerability:** Binary classification systems (sanctioned/non-sanctioned) used in the OFAC list exhibit inherent vulnerabilities to *dusting attacks*, where small amounts of sanctioned funds are strategically distributed to arbitrary addresses. Our analysis reveals that 12 ETH from sanctioned services were used to dust addresses controlling over 9 million ETH within 48 hours after sanctions took effect.
(2) **Partial Sanction Enforcement:** Only 19.11% of blocks are generated by block producers that actively enforce sanctions, and even these producers only filter direct interactions rather than subsequent fund movements. This enforcement gap has enabled more than 1 million ETH to be processed by the sanctioned mixing service, with these funds subsequently circulating through various services on Ethereum.
(3) **Comprehensive Obfuscation Ecosystem:** Users leverage the entire Ethereum service landscape to obscure fund origins, including Decentralized Exchange (DEX), Centralized Exchange (CEX), cross-chain bridges, alternative privacy-enhancing tools (e.g., Umbra [34] and Railgun [33]), and other platforms.

Using TC as a case study, we quantitatively analyze how sanctions affect user behaviors and service usage across the blockchain ecosystem. The key contributions of this work include:

- **Advanced Scoring and Tracking Algorithm:** We introduce a more practical tracking algorithm that uses a quantitative impurity metric to precisely measure the propagation and concentration of sanctioned funds throughout the Ethereum ecosystem. We provide arguments to claim that the naïve binary classification method used by OFAC sanctions is vulnerable to dusting attacks.

[*] Co-supervised this research project.

By integrating Ethereum's state transition function, our implementation incrementally computes impurity metrics as transactions modify account balances. This approach achieves an average processing time of 0.07 ± 0.03 seconds per newly appended block during node synchronization, meeting real-time monitoring requirements across Ethereum Virtual Machine (EVM)-compatible chains. We further validate our approach against addresses in public Bybit exploiter datasets [12, 15] as the proxy ground truth, achieving 97.61% precision and 74.08% recall.

- **Empirical Sanction Effectiveness Analysis:** We empirically evaluate the effectiveness of OFAC sanctions on TC across a comprehensive dataset spanning 957 days of the entire sanction period, encompassing 6.79 million blocks and 1.07 billion transactions. Our findings indicate that, although the overall TC deposit volume decreased by 71.03% during the sanction period compared to an equivalent pre-sanction timeframe, TC remains the primary tool for laundering malicious proceeds in Ethereum-related security incidents. Moreover, we highlight gaps in sanction enforcement performed by block producers, which allows sanctioned assets to continue propagating.
- **Empirical Insights into Evasion Techniques:** Our tool can detect notable user strategies, such as *split-and-merge* patterns (associated with money laundering) and *test-depositing* transactions (used to probe sanction enforcement policies). We systematically characterize user behaviors when interacting with service providers. To improve our cross-chain analysis, we additionally implement parsers supporting 20 bridges and 2 proxy aggregators, enabling extraction of destination chain identifiers and recipient addresses. Beyond security incidents funded via TC, we uncover the workflows behind rug-pull and address-poisoning scams that use TC to obscure their fund origins. The quantitative results serve as actionable insights and policy recommendations for regulatory authorities and compliance teams, enabling them to better detect and mitigate malicious activities. All datasets and code modules are publicly available to support future research.

## 2 BACKGROUND

This section outlines the necessary background for the paper.

*Ethereum and Its Service Ecosystem.* Ethereum is a decentralized blockchain system that supports smart contracts – programs that can be deployed and executed by anyone on the network. Unlike Bitcoin's Unspent Transaction Output model [25], Ethereum employs an account-based model where each address maintains a state including its balance and other attributes [45]. The native cryptocurrency, Ether (1 ETH = $10^{18}$ Wei), serves both as a medium of exchange and as "gas" to pay for all computational operations within the network. Transactions are processed by miners (Proof-of-Work) or validators (Proof-of-Stake after the "Merge" in Sep. 2022), who receive rewards for including transactions. The Ethereum ecosystem encompasses a diverse range of services:

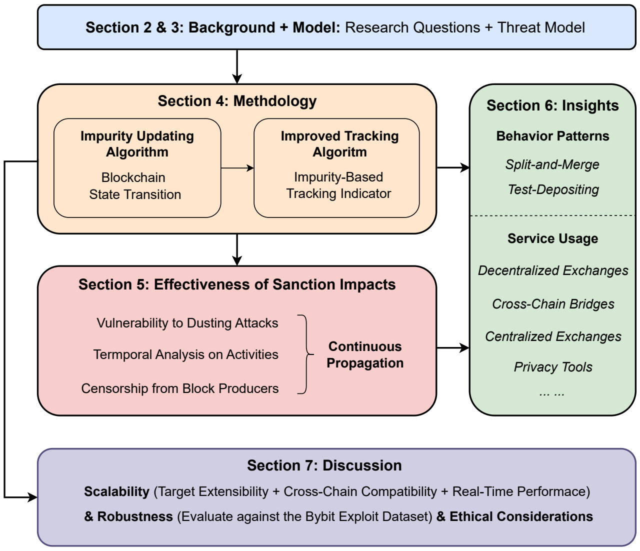

Section 2 & 3: Background + Model: Research Questions + Threat Model
Section 4: Methdology
Impurity Updating Algorithm
Blockchain State Transition
Improved Tracking Algoritm
Impurity-Based Tracking Indicator
Section 6: Insights
Behavior Patterns
Split-and-Merge
Test-Depositing
Service Usage
Decentralized Exchanges
Cross-Chain Bridges
Centralized Exchanges
Privacy Tools
... ...
Section 5: Effectiveness of Sanction Impacts
Vulnerability to Dusting Attacks
Termporal Analysis on Activities
Censorship from Block Producers
Continuous Propagation
Section 7: Discussion
Scalability (Target Extensibility + Cross-Chain Compatibility + Real-Time Performace)
& Robustness (Evaluate against the Bybit Exploit Dataset) & Ethical Considerations

**Figure 1: Section 3 introduces our research questions and threat model. Section 4 describes the impurity updating algorithm and our enhanced tracking methodology. In Section 5, we evaluate the effectiveness of sanctions, examining phenomena such as dusting and partial on-chain censorship. Section 6 offers additional insights into behavioral patterns and service usage. Finally, Section 7 addresses scalability, robustness, ethical considerations and limitations.**

**Privacy-Enhancing Tools**: Mixing services like TC aim to break the on-chain linkability between deposit and withdrawal transactions. It operates via fixed-denomination mixing pools (0.1 ETH, 1 ETH, 10 ETH, and 100 ETH), utilizing Zero-Knowledge Proofs to provide a cryptographic proof of commitment ownership without revealing specific commitments. Other tools like Umbra [34] and Railgun [33] leverage stealth addresses to prevent observers from connecting multiple payments to the same entity. While these tools serve legitimate privacy needs, they fundamentally challenge traditional regulatory approaches.

**Exchanges**: There are two primary types of cryptocurrency exchanges. DEX like Uniswap [37] and 1inch [1] operate entirely on-chain through smart contracts, enabling peer-to-peer trading without custodial intermediaries. Most operate through an Automated Market Maker (AMM), which use mathematical formulas to price assets based on the ratio of tokens in liquidity pools. CEX such as Binance [6] and Coinbase [9] function as traditional financial intermediaries, maintaining order books, and custodying user funds. CEXs act as gateways between fiat and crypto, typically enforcing different levels of compliance requirements.

**Cross-Chain Bridges**: Services that facilitate asset transfers between different blockchain networks to expand interoperability. Unlike token standards (e.g., ERC-20 [14]) which provide consistent interfaces, cross-chain bridges lack standardization in their implementation, message formats, and identifier systems. The differences in their architectures [3] create significant technical challenges for cross-chain transaction monitoring and fund tracing.

**Other DeFi Services**: Applications in DeFi providing lending, Non-Fungible Token (NFT) trading, and other financial services through smart contracts without traditional intermediaries [44].

*Regulatory Frictions.* The pseudonymous and decentralized nature of blockchains challenges traditional censorship frameworks.

**Regulatory Evolution**: Traditional Anti-Money Laundering (AML) and Counter-Terrorism Financing (CTF) frameworks require Know-Your-Customer (KYC) for customer identification and Know-Your-Transaction (KYT) for transaction monitoring. The Financial Action Task Force (FATF) has extended these requirements to virtual asset service providers through recommendations like the "Travel Rule" [16], which conflicts with blockchain's pseudonymous design.

**Blockchain Sanctions**: The U.S. OFAC has expanded their sanctions regimes to include specific blockchain addresses and services. Sanctions on TC in August 2022 targeted an autonomous smart contract system that is abused to launder over 7 billion USD worth of cryptocurrency, including over 455 million USD stolen by the North Korean state-sponsored Lazarus Group [38]. This action classifies privacy technology itself as a compliance risk, marking a significant escalation in regulatory response to blockchain privacy tools. As a result, recent work [4, 20, 48] and protocols [33, 50] consider compliance requirements in their designs and implementations.

**Enforcement Through Multiple Vectors**: The decentralized nature of blockchain systems has necessitated multi-layered censorship approaches that operate at different levels of the technology stack: *(i)* block producers can refuse to include transactions involving sanctioned addresses [40], *(ii)* user interfaces and front-ends of DeFi applications can block addresses that interact with sanctioned services, and *(iii)* stablecoin providers and centralized services can freeze assets or close accounts based on their blacklist mechanisms.

## 3 MODEL

This section presents our research questions and threat model, developed in the context of Ethereum but broadly applicable to other EVM-compatible chains that follow the account-based model.

### 3.1 Problem Statement

Regulatory bodies such as OFAC regularly publish sanctions targeting certain blockchain addresses to limit criminal financing, money laundering, and other malicious activities. However, the pseudonymous, permissionless, and composable nature of blockchains introduces new challenges in effectively enforcing these restrictions. In this paper, we aim to systematically study the effectiveness of sanctions and answer the following research questions:

- ***RQ1.*** *How can on-chain analysis techniques robustly detect sanctioned addresses (and derived addresses) with scalability and real-time performance?* (**cf. Section 4, Finding 5.1**)
- ***RQ2.*** *How do benign and malicious blockchain participants react to sanctions?* (**cf. Section 5, Findings 5.2 and 5.3**)
- ***RQ3.*** *To what extent do these sanctioned addresses or sanctioned service users exploit additional tactics to complicate detection?* (**cf. Section 6, with quantitative analysis**)

We consider TC on Ethereum as a case study to illustrate the effectiveness of our design and analysis. Its recent removal from the OFAC sanctions list [39], coupled with large-scale transactions recorded during the sanction period, provides a stable, complete, and immutable dataset. This allow us to systematically examine the entire lifecycle of sanction events (from initial imposition to eventual delisting) in a controlled environment. Unlike ongoing sanction cases subject to evolving conditions, the finalized status of TC ensures data consistency and integrity, enabling rigorous analyses of user behaviors and sanction effectiveness. By leveraging this dataset, we can derive data-driven recommendations to inform future regulatory strategies across decentralized finance platforms.

### 3.2 Threat Model

We consider adversaries who aim to conceal fund flows originating from sanctioned sources. These adversaries may range from individual actors to state-backed organizations (e.g., Lazarus Group). We assume they have full visibility of the blockchain's public data and can undertake the following on-chain actions:

- **Dusting:** Adversaries can send arbitrary amounts to random addresses (including innocent accounts) to create ambiguous connections and inflate the scale of transaction tracing graphs, making it more difficult to pinpoint the true flow of funds.
- **Layering:** Adversaries can generate an unrestricted number of addresses and transactions to split (from one source to multiple destinations) or merge (from multiple sources to one destination) their assets. Furthermore, these addresses can be used only once to undermine straightforward clustering heuristics.
- **Interacting:** Adversaries can create their own smart contracts and can interact with any deployed on-chain service, including swapping tokens on DEX, cashing out via CEX, bridging to other blockchains, using privacy-enhancing tools, or engaging with DeFi lending and NFT trading platforms.

We assume that adversaries cannot compromise the blockchain's cryptographic foundations, exploit previously unknown smart contract vulnerabilities, or conspire with a majority of block producers or service providers. Our primary goal and focus is to expose the behavioral patterns of adversaries and the ultimate destinations of assets once they leave malicious or sanctioned accounts.

## 4 METHODOLOGY

In this section, we provide a formal description of our framework for tracking sanctioned funds, focusing on three key components: notations and definitions, an iterative procedure for updating the impurity scores, and our improved tracking algorithm that leverages these scores to manage the scope of the tracking and analysis.

### 4.1 Notations and Definitions

To ease the understanding of the following paragraphs, we proceed by introducing the following notations and definitions.

**Address** $addr \in ADDR$, where $ADDR$ is the set of all valid 160-bit Ethereum addresses. We use the terms "address" and "account" interchangeably as each account is identified by a unique address, referring to externally owned accounts and smart contract accounts.

**Sanctioned Address Set** $ADDR_{Sanction} \subset ADDR$.

**Blockchain State** $s \in \mathcal{S}$ includes *(i)* the state of all accounts (e.g., balance and transaction nonce), *(ii)* the state of all smart contracts, and *(iii)* blockchain metadata (e.g., block numbers, timestamps, miner addresses, gas used, gas price, etc.) at a given point in time.

**Operation** $op \in OP$, where $OP$ is the set of operations that modify the blockchain state $s$ (e.g., asset transfers and contract invocations).

**Balance Function** $\mathcal{B}(s, addr) \rightarrow \mathbb{N}_0$ returns the non-negative integer balance (in Wei) for a given address $addr$ in state $s$.

**State Transition** $\mathcal{T}(s, op) \rightarrow s'$ returns the new state $s'$ after the current state $s$ applies operation $op$. Specifically, given a balance operation $op_{\mathcal{B}}$ that affects addresses $\{addr_{from}, addr_{to}\} \subset ADDR$ and amounts $\{a_{sent}, a_{received}\} \subset \mathbb{N}_0$, such that

$$op_{\mathcal{B}} \rightarrow \{\, \langle addr_{from}, a_{sent}\rangle, \langle addr_{to}, a_{received}\rangle \,\}$$

the balance state transition $\mathcal{T}_{\mathcal{B}}$ is

$$\mathcal{B}(s', addr_{from}) = \mathcal{B}(s, addr_{from}) - a_{sent}$$
$$\mathcal{B}(s', addr_{to}) = \mathcal{B}(s, addr_{to}) + a_{received}$$

**Impurity Function** $\mathcal{I}(s, addr) \rightarrow \mathbb{N}_0$ returns the non-negative integer amount originated from $ADDR_{Sanction}$ in balance (in Wei) for a given address $addr$ in state $s$, such that

$$0 \le \mathcal{I}(s, addr) \le \mathcal{B}(s, addr)$$

**Impurity Score** $\varphi(s, addr)$ is defined as

$$\varphi(s, addr) = \begin{cases} \frac{\mathcal{I}(s,addr)}{\mathcal{B}(s,addr)}, & \text{if } \mathcal{B}(s, addr) > 0 \\ 0, & \text{if } \mathcal{B}(s, addr) = 0 \end{cases}$$

By definition, $\varphi(s, addr) = 0$ indicates there is no traceable connection between $addr$ and $ADDR_{Sanction}$ or no balance under $addr$ at the state $s$, and $\varphi(s, addr) = 1$ shows that all balances under $addr$ are traceable to sanctioned addresses at the state $s$. This score provides a relative measure of an address's historical association with sanctioned outflows. It is important to note that this approach aligns with Ethereum's account model, where the impurity of funds can be treated as an extra state or property of an Ethereum address.

## 4.2 Impurity Updating Algorithm

Our impurity updating algorithm (cf. Appendix B) operates on the following inputs: blockchain states $\{(s_0, s_1, \ldots, s_{n-1}) \mid s \in \mathcal{S}\}$, a set of operations $OP_{\mathcal{B}}$ that causes the transition of balance state, a set of all Ethereum addresses $ADDR$, and a set of sanctioned addresses $ADDR_{Sanction}$. The algorithm then identifies the operation type, extract the affected addresses and corresponding amounts, consequently updating their impurity $\mathcal{I}$ from state $s$ to $s'$. The algorithm output is historical records of $\langle \mathcal{I}, \mathcal{B}, \varphi \rangle$ for all involved addresses at each block. Our algorithm includes the following phases:

(1) **Initialization:** Let $s_0 = s_{OFAC}$, where $s_{OFAC}$ is the blockchain state immediately after the OFAC sanction took effect. For each address $addr \in ADDR_{Sanction}$, we set

$$\mathcal{I}(s_{OFAC}, addr) = \mathcal{B}(s_{OFAC}, addr)$$

For all other addresses $addr \notin ADDR_{Sanction}$, we initialize

$$\mathcal{I}(s_{OFAC}, addr) = 0$$

(2) **State Transition.** Given a state pair $(s_i, s_{i+1})$, we extract the balance-related operation $op_{\mathcal{B}}$ from the corresponding balance state transition $\mathcal{T}_{\mathcal{B}}(s_i, op_{\mathcal{B}}) \rightarrow s_{i+1}$, alongside the affected addresses and amounts $\{\, \langle addr_{from}, a_{sent}\rangle, \langle addr_{to}, a_{received}\rangle \,\}$. The $op_{\mathcal{B}}$ has the following types:

- **Transaction Fee**, which is the cost that transaction senders $addr_{from} = addr_{sender}$ pays to have their transactions processed and included in a block by some block producer (miner or validator) $addr_{to} = addr_{producer}$. It includes the calldata fee and blob fee. It is worth noting that after the London Hard Fork (EIP-1559), part of the fee is burnt because of deflationary pressure, so $a_{sent} > a_{received}$.
- **Value Transfer**, which refers to the process of moving assets (i.e., ETH) from one account ($addr_{from}$) to another ($addr_{to}$), and $a_{sent} = a_{received}$. We use Geth Debug APIs to track each call frame and consider only those that change the balance state. Therefore, call frames with zero transfer values, `CallCode` (also its replacement `DelegateCall`) and `StaticCall` are ignored.
- **Reward**, which indicates the incentive given to block producers for contributing resources to maintain and secure the network. Let $s_{PoS}$ be the blockchain state when the PoS merge happened (Block 15537394). For states before $s_{PoS}$, rewards are distributed to miners and uncles ($addr_{to} = addr_{miner}$). At and after $s_{PoS}$, only Beacon withdrawals to validators ($addr_{to} = addr_{validator}$) are considered. Since there is no from address ($addr_{from}$ = NULL, $a_{sent} = 0$), We assume that all rewards and withdrawals are irrelevant to $ADDR_{Sanction}$.

(3) **Impurity Update.** Given the state pair $(s_i, s_{i+1})$ with extracted addresses and amounts $\{\, \langle addr_{from}, a_{sent}\rangle, \langle addr_{to}, a_{received}\rangle \,\}$, the impurity $\mathcal{I}$ can be updated as:

$$\mathcal{I}(s_{i+1}, addr_{from}) = \mathcal{I}(s_i, addr_{from}) - \left\lceil \frac{a_{sent} \cdot \mathcal{I}(s_i, addr_{from})}{\mathcal{B}(s_i, addr_{from})} \right\rceil$$

If $addr_{to} \in ADDR_{Sanction}$, which means assets are sent back to the sanctioned addresses:

$$\mathcal{I}(s_{i+1}, addr_{to}) = \mathcal{B}(s_{i+1}, addr_{to})$$

Otherwise when $addr_{to} \notin ADDR_{Sanction}$:

$$\mathcal{I}(s_{i+1}, addr_{to}) = \mathcal{I}(s_i, addr_{to}) + \left\lceil \frac{a_{received} \cdot \mathcal{I}(s_i, addr_{from})}{\mathcal{B}(s_i, addr_{from})} \right\rceil$$

(4) **Repeat:** Continue applying the **2) State Transition** and **3) Impurity Update** for each subsequent state pairs. It is worth noting that a block transition is simply a series of these state transitions in this block applied sequentially.

## 4.3 Improved Tracking Algorithm

In this section, we present our refined strategy for tracking assets withdrawn from TC to counter two key challenges arising from the differences with the post-incident investigation.

*4.3.1 Identification of TC Withdrawers.* Typical incident-driven investigations [17, 46] identify a small set of attacker-controlled addresses that issue malicious transactions, usually through victims or third-party security services. However, TC withdrawers need to be extracted from continually generated withdrawal transactions.

We begin by identifying the TC ETH contracts, cross-referencing the OFAC sanction list [7] and verified labels from established research [40, 43]. Two notable obfuscation strategies complicate the direct linkage between TC contracts and withdrawers. First, TC relayers often submit transactions on behalf of users, further concealing the link between depositors and withdrawers. Newly created withdrawal addresses, which typically lack sufficient balances to cover gas fees, rely on these relayers to execute the actual transactions on-chain. Consequently, in transaction records, the relayer address appears as the one interacting with TC contracts rather than the true beneficiary. Second, a sequence of newly deployed smart contracts can delegate calls from one contract to the next until reaching the TC contracts, masking direct interactions.

To deal with these two obfuscations, we perform an in-depth inspection of transaction logs using the `eth.get_logs()` function on our local Ethereum archive node. Even if the relayer address or the newly created proxy contracts appear in the sender or receiver fields, the `data` field in withdrawal topic exposes the genuine beneficiary addresses and withdrawn amounts. By meticulously extracting this information, we can reliably capture all addresses and amounts derived from TC withdrawal transactions. It is worth noting that this method can be extended to tracking withdrawers from any sanctioned smart contracts.

*4.3.2 Impurity-based Tracking Indicator.* Following TC outflows quickly leads to an exponential number of addresses and transactions to be tracked because each address can branch to multiple recipient addresses in transactions. Therefore, establishing appropriate termination criteria to prevent transaction graph explosion during analysis becomes crucial. Post-incident traces [46] commonly assume a limited hop number or short money laundering time window, which means attackers are likely to move stolen funds swiftly. Under such time-pressured conditions, analysts ignore smaller-scale suspicious flows that deviate from the primary transaction path. However, TC-related activities do not need to adhere to such condensed timelines. These anonymous funds can remain dormant across multiple addresses indefinitely. This persistence undermines analytical approaches that rely on simplistic cutoffs in hop count, time window, or transaction value.

To address this broader threat landscape, we incorporate the impurity-based terminating indicator into our tracking pipeline. Specifically, we compute an *impurity score* $\varphi$ for each observed address (cf. Section 4.1 and 4.2). We then derive a threshold $\Phi$ from the overall distribution of impurity scores (cf. Section 5.4) and the algorithm evaluation against the Bybit exploit (cf. Section 7.2). This threshold aims to capture any address exhibiting suspicious mixing characteristics, including those sending or receiving zero- or small-value transfers that conventional cutoffs might miss. Moreover, in scenarios involving *super-accounts* (i.e., addresses with thousands of transactions or more in history) with high-impurity ($\varphi \geq \Phi$), tracking does not terminate. Instead, these addresses are flagged for deeper scrutiny. The process will halt when tracking becomes *highly irrelevant* (where $\varphi < \Phi$) or *highly improbable* (where on-chain linkability is broken, e.g., funds enter privacy-enhancing tools). It is worth noting all subsequent transactions from the latter case are pruned from the transaction graph.

## 5 EFFECTIVENESS OF SANCTION IMPACTS

To examine the effectiveness of OFAC sanctions on TC, we conduct a comprehensive evaluation using historical Ethereum blockchain data. Our analysis covers the entire sanction period from Block 15302392 ($s_{OFAC}$, August 8, 2022) to block 22097863 ($s_{END}$, March 21, 2025) with 6.79 million blocks and 1.07 billion transactions.

### 5.1 Dusting Behaviors

Following the announcement of OFAC sanction on TC, a significant dusting attack emerged: small amounts of ETH were deliberately withdrawn from TC to a wide range of addresses. Our analysis focused on transactions from the smallest TC 0.1 ETH mixing pool within 14,400 blocks (approximately 48 hours) after $s_{OFAC}$. The dusting targets included prominent entities like Ethereum Foundation, CEX (e.g., Kraken, Binance, Bitfinex, Gemini, OKX, etc.), and random users interacting with DeFi platforms. These dusting attacks effectively flagged numerous unsuspecting recipients as potentially sanctioned or involved in malicious activities.

**Table 1: Impact of the Sanction on TC: while withdrawal volume also declined significantly (-66.80%), they remained slightly higher than deposit volumes (-71.03%), suggesting users prioritized exiting over continued use.**

| Metric | Action | Pre-$s_{OFAC}$ | Post-$s_{OFAC}$ | Change |
|---|---|---|---|---|
| # Transaction | Deposit | 150,403 | 42,753 | -71.57% |
| | Withdraw | 139,404 | 44,283 | -68.23% |
| # Address | Deposit | 39,397 | 9,175 | -76.71% |
| | Withdraw | 58,567 | 20,734 | -64.60% |
| Volume (in ETH) | Deposit | 3.49M | 1.01M | -71.03% |
| | Withdraw | 3.27M | 1.08M | -66.80% |

A direct consequence of these dusting behaviors was the Denial-of-Service attack on services (e.g., Aave Front-End [2]) using the binary classification mechanism. We observed that dusters used merely 12.00 ETH to taint at least 9,034,251.58 ETH (over $750,000\times$) belonging to the affected recipients. This significantly increased the risk of asset freezing and service denial by compliant platforms. The dusting phenomenon underscores the need for continuous and quantitative risk metrics, such as our proposed impurity scores $\varphi$, that can capture varying levels of exposure to sanctioned funds. Such metrics enable regulators and service providers to implement proportional compliance responses based on precise risk assessments, rather than naïve binary classifications.

***Finding 5.1 - See Appendix C for Detailed Arguments***

***Naïve binary classification cannot be resistant against dusting attacks. Combating dusting attacks requires a quantitative approach.***

### 5.2 Temporal Analysis

Table 1 presents our quantitative analysis of how OFAC sanctions affected TC. We observed a significant decrease in overall usage, yet found that the sanction had limited impact on attacks.

*5.2.1 Reduction in Post-Sanction Activity.* We extended the previous study of Wang et al. [43], by examining a comprehensive dataset spanning 966 days before and 957 days after the OFAC sanctions on TC. Table 1 shows a substantial reduction in the number of transactions, unique addresses, and total volumes for both TC deposits and withdrawals. Specifically, post-sanction deposit volume fell to only **28.97%** of pre-sanction levels when comparing equivalently long time periods. Figures 2 displays the daily statistics for deposits and withdrawals. Following the announcement of the sanctions, we observed a significant increase in withdrawal transactions (labeled as Peak Ⓟ ). This peak represents the highest daily withdrawal transaction count after OFAC sanctions and also indicates a mass

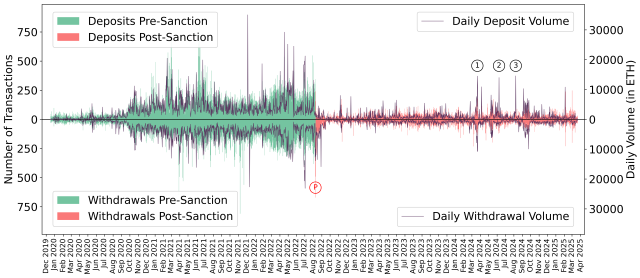

**Figure 2: Daily transactions and volumes into the TC ETH pools from December 16, 2019 to March 21, 2025. The x-axis denotes the timeline, while the y-axis captures transaction count and volume of deposits (up) and withdrawals (down). The three circled values mark the top-3 post-sanction daily deposit volumes, each linked to a known security incident. Moreover, a significant spike in withdrawals is observed on the sanction date, marked by the circled letter "P".**

exodus from TC, suggesting that users were prompted to withdraw their assets due to heightened uncertainty.

*5.2.2 Limited Effect on Attackers.* We took a snapshot of the BlockSec database [1] as of March 21, 2025. This dataset catalogs significant DeFi exploits with losses exceeding 100,000 USD and provides one of the most comprehensive public records of major attacks. Of the **80** total incidents in the dataset, funds were returned to victims in 9 cases. Among the remaining **71** malicious attacks, attackers in 11 cases retained stolen assets by converting them to non-freezable cryptos (e.g., ETH or DAI). Notably, among the **60** incidents with active money laundering activity, attackers used TC as their primary laundering method in **47 cases (78.33%)**. Moreover, we observed that in **35 (49.30%)** out of these **71** malicious incidents, attackers sourced their funding from TC to facilitate the exploit transactions. Importantly, **29 (82.86%)** of these **35** cases subsequently returned stolen assets back into TC, further obfuscating on-chain footprints.

Moreover, we identified three significant deposit peaks after the sanction date, as illustrated in Figure 2. The first peak, denoted as Peak ①, occurred on March 21, 2024, predominantly driven by the Heco Bridge Exploiter [28], who contributed 11,200.00 ETH, representing **77.11%** of the total deposits (14,522.00 ETH) on that day. The second peak, Peak ②, took place on June 8, 2024, with deposits primarily originating from the Orbit Bridge Exploiter [29]. This attacker deposited 12,930.00 ETH, accounting for **92.18%** of the day's total deposit volume (14,027.00 ETH). The third and most pronounced peak, Peak ③, was recorded on August 8, 2024, with the Nomad Bridge Exploiter [27] depositing 14,509.30 ETH, constituting nearly the entirety (**99.50%**) of the day's total 14,581.70 ETH.

***Finding 5.2***

***OFAC sanctions on TC significantly reduce general user activity but fail to deter malicious actors.***

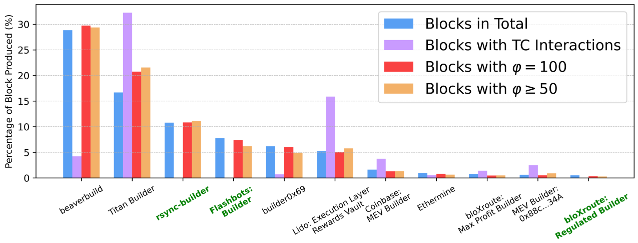

**Figure 3: Top block producers on Ethereum between $s_{OFAC}$ and $s_{END}$. Blocks with TC interactions (purple) represent blocks that contain direct deposits and withdrawals with four TC ETH pools. Blocks with score conditions (red and yellow) indicate blocks that include transactions issued by accounts that meet the condition. Note that rsync-builder, Flashbots: Builder, and bloXroute: Regulated Builder (in green) follow OFAC sanctions to reject direct TC interactions.**

## 5.3 Censorship from Block Producers

Previous research [40] showed that block producers can and do filter out transactions associated with OFAC-sanctioned entities to avoid including them in their blocks. These censorship behaviors can be driven by external pressures (e.g., regulations) or internal motivations (e.g., ethical or economic considerations). However, our re-evaluation of block producer behaviors using the proposed impurity score $\varphi$ revealed a significant discrepancy between direct censorship and indirect handling of downstream funds.

As illustrated in Figure 3, three notable block producers, rsync-builder, Flashbots: Builder and bloXroute: Regulated Builder, actively follow OFAC sanctions. The rsync-builder demonstrated the most rigorous censorship. It produced 734,343 blocks (10.81% of a 6.79 million block sample between $s_{OFAC}$ and $s_{END}$) without including any direct interactions with four TC ETH pools. However, our analysis of blocks containing senders with high impurity scores ($\varphi = 100\%$ and $\varphi \geq 50\%$) revealed that rsync-builder produced these blocks at rates (10.83% and 11.10%, respectively) that closely match its overall block production rate (10.81%). We observed similar patterns with Flashbots: Builder and bloXroute: Regulated Builder. This consistency demonstrated a critical finding: block producers that rigorously censored direct TC interactions failed to scrutinize transactions involving addresses that previously received TC funds. This highlights a significant gap in their sanction enforcement. Figure 12 in Appendix F further records the historical impurity amount and score for rsync-builder where impurity scores can reach $\varphi \approx 70\%$. The remaining 8 block producers only partially complied or did not enforce OFAC sanctions, such as Titan Builder which contributed the largest proportion (32.24%) of blocks in which exist transactions that directly interacted with TC. Meanwhile, beaverbuild led in the number of blocks meeting certain impurity conditions, aligning proportionally with its overall block production.

Block producers derive significant revenue beyond transaction fees and block rewards from Maximal Extractable Value (MEV). In this process, MEV bots pay block producers for favorable transaction placement, enabling profitable strategies such as arbitrage [32].

[1] https://docs.blocksec.com/phalcon/security-incident-list

Our investigation revealed that some of these MEV operations received funding from TC, as evidenced by bots like 0x06e8...c9fc and 0x0000...266C. This further raises critical compliance concerns, as block producers may unintentionally facilitate the movement of sanctioned assets, exposing themselves to regulatory risks.

***Finding 5.3***

***Only a subset of block producers follow OFAC sanctions, and they only censor direct TC deposit and withdrawal transactions. Furthermore, major block producer does not scrutinize post-TC transactions.***

## 5.4 Impurity Distribution

This section analyzes the distribution of TC-derived funds in the Ethereum ecosystem, focusing on the impurity levels of fund holders, measured by both impurity scores $\varphi$ and amounts $\mathcal{I}$.

*5.4.1 General Distribution.* We conducted a comprehensive analysis on approximately 67.94 million addresses holding funds that could have originated from TC at $s_{END}$. Table 2 first shows that more than 99% of addresses have impurity scores below 5% ($\varphi < 5\%$). These addresses represent 99.62% of the total balance amounts and contain 76.05% of all impurity amounts, suggesting widespread but relatively low-level contamination across the vast majority of affected addresses. Typical Ethereum ecosystem operations primarily explain this prevalence. For instance, CEX hot wallets aggregate funds from numerous users, inevitably including some originating from TC. As a result, these CEX user addresses inevitably acquire low impurity scores through subsequent operations. We then investigated the addresses having impurity scores that exceed 95% ($\varphi \geq 95\%$). Although these addresses constitute merely 0.07% of the total population and 0.20% of the total balance amounts, they disproportionately account for 21.91% of all impurity amounts.

We further analyzed addresses with intermediate impurity scores ($5\% \leq \varphi < 95\%$), using 50% as an extra dividing point. This dividing point clearly distinguishes addresses with predominantly normal funds from those primarily containing TC-derived assets. Addresses with impurity scores between 5% and 50% constitute 0.83% of total addresses and hold just 1.68% of the entire impurity amounts. The addresses between 50% and 95% impurity are even rarer (0.02%) and contain merely 0.36% of all impurity amounts.

Table 2 summarizes the distribution of addresses and impurity amounts according to the impurity scores. For our initial analysis, we set the impurity threshold $\Phi = 5\%$ as the terminating indicator (cf. Section 4.3.2). However, it is important to note that this threshold is not a definitive recommendation but serves primarily as an experimental baseline for Section 6, as evaluating its efficacy requires ground truth data which is not universally available. The selection of an appropriate threshold involves inherent trade-offs that merit careful consideration. A lower threshold increases sensitivity but potentially introduces more false positives, necessitating additional manual verification resources. Conversely, a higher threshold may reduce false alarms but risks missing malicious activities (false negatives). In practice, regulators and compliance teams should calibrate this parameter according to their operational constraints, risk tolerance, and available resources (potentially in conjunction with complementary metrics to enhance accuracy). We further explore this threshold-performance relationship through a case study of the Bybit exploit in Section 7.2, where ground truth data enables a more rigorous evaluation of different threshold configurations.

**Table 2: Distribution of Addresses with their Impurity Amounts and Total Balance Amount by Impurity Scores $\varphi$**

| **Score $\varphi$** | **# Address** | **Impurity Amount $\mathcal{I}$** | **Total Balance Amount $\mathcal{B}$** |
|---|---|---|---|
| [ 0%, 5% ) | 67,321,336 (99.08%) | 877,243.20 ETH (76.05%) | 127,696,284.34 ETH (99.62%) |
| [ 5%, 50% ) | 560,858 (00.83%) | 19,363.70 ETH (01.68%) | 224,987.50 ETH (00.18%) |
| [ 50%, 95% ) | 16,665 (00.02%) | 4,155.41 ETH (00.36%) | 5,832.83 ETH (00.00%) |
| [ 95%, 100% ] | 45,258 (00.07%) | 252,763.76 ETH (21.91%) | 252,812.50 ETH (00.20%) |
| **Total** | 67,944,117 (100%) | 1,153,526.07 ETH (100%) | 128,179,917.19 ETH (100%) |

*5.4.2 Top Impurity Amount Holders.* To identify key concentration points of TC-derived funds, we analyzed the top-20 accounts ranked by impurity amounts $\mathcal{I}$ at $s_{END}$, as shown in Table 5 (Appendix F). Our analysis revealed that over 55.31% of the funds withdrawn from TC had been integrated into various services on Ethereum. Ethereum 2.0 staking, DEX, CEX, cross-chain bridges, and other DeFi services are popular destinations. Identifying these concentration points enables more targeted regulation and provides essential context for the fund flow analysis presented in Section 6.2.

# 6 INSIGHTS INTO FUND FLOWS

In this section, we present detailed insights into how funds flow after withdrawals from TC. Specifically, we focus on two primary aspects: first, behavioral patterns of TC withdrawers prior to depositing into services; and second, their subsequent interactions with various service providers. Through this analysis, we aim to enhance the understanding of user strategies and support efforts in tracing sanction-related activities across blockchain ecosystems.

## 6.1 Behavioral Patterns

Between the initial withdrawal from TC and subsequent deposit into Ethereum services, we identify and analyze two primary behavioral patterns: *split-and-merge* and *test-depositing*.

*6.1.1 Split-and-Merge Pattern.* We apply our scoring and tracking algorithms to both TC withdrawers and the Bybit exploiter. Our comparative analysis, as shown in Figure 8 (Appendix A), reveals their behavioral similarities between these actors based on the frequency of connected three-node motifs [5]. We can also observe this pattern in the complex transaction graph of the Bybit exploit rendered by our front-end tool in Figure 7 (Appendix A).

The *split-and-merge* pattern emerges as a distinctive signature, characterized by entities initially splitting funds across multiple addresses (Motif 021D), transferring them through intermediate addresses (Motif 021C), and finally merging assets (Motif 021U). This technique is specially designed to circumvent transaction monitoring systems and has been documented in both traditional and crypto-specific money laundering studies. This behavioral similarity, combined with widespread usage of TC following security incidents (cf. Section 5.2.2), further raises concerns about TC's significant role in crypto money laundering operations.

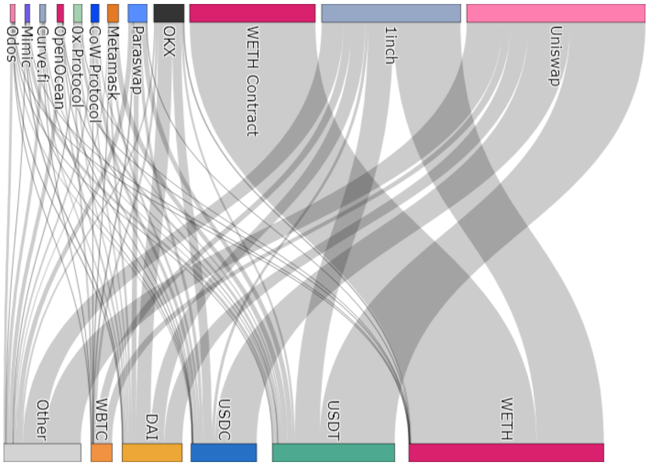

**Figure 4: Flow of Funds via Decentralized Exchanges. Over 86.27% of impurity volume are swapped into stablecoins and wrapped tokens. Notably, USDT and USDC have blacklist mechanisms to freeze assets held by sanctioned entities.**

*6.1.2 Test-Depositing Sequences.* Another behavior involves conducting small exploratory deposits before committing to substantial transfers. Figure 13 in Appendix F illustrates this behavior: a user first deposited around 0.1 ETH to KuCoin, then consistently transferred larger amounts (10-12 ETH) in all subsequent transactions.

This sequential approach serves three specific risk-mitigation purposes. First, users validate that their accounts remain operational within sanction-compliant systems. Second, they confirm that automated compliance screening does not flag their transactions. Third, they verify the receiving platform's regulatory controls do not impose restrictions on their activities. Our analysis of five services implementing regulatory requirements reveals a precise proportion: 38.55% of Binance, 75.31% of Railgun, 49.02% of OKX, 47.73% of Gate.io, and 46.59% of KuCoin users, who execute multiple deposits, demonstrate this test-then-transfer sequence. In contrast, platforms without sanctions enforcement exhibit different patterns. Users interacting with these services typically skip the testing phase, preferring to transfer substantial amounts in single transactions through primarily one-time intermediate addresses. This behavioral difference creates a detectable marker that financial intelligence units and compliance systems can leverage.

## 6.2 Service Usage

Following our examination of behavioral patterns, we investigated the diverse service providers that TC withdrawers commonly use. This section highlights five primary categories: DEX, cross-chain bridges, CEX, privacy-enhancing tools, and miscellaneous services.

*6.2.1 Decentralized Exchanges.* DEX emerge as one significant choice utilized by sanctioned addresses, accounting for 26.78% of all impurity volume $\mathcal{I}_v$ in our database. This preference stems from their permissionless architecture and censorship-resistant design. DEX also serve as gateways for swapping ETH into different tokens required for subsequent obfuscation steps.

**Service Providers.** Our tracking algorithm identified transactions flowing into more than 12 DEX platforms as shown in the upper side of Figure 4. Among these platforms, Uniswap [37] (33.04%) and 1inch [1] (25.64%) dominated DEX activities on Etherum. Although their official websites profess compliance with sanctions and implement front-end filters, these measures can be circumvented through directly on-chain contract invocations. Consequently, large volumes of TC-derived funds ($\mathcal{I}_v = 289,901.92$ ETH) still flowed into platforms. Specifically, we observed that 102,928.18 ETH (impurity score $\varphi \approx 93.04\%$) channeled through Uniswap and 77,481.93 ETH ($\varphi \approx 95.95\%$) processed via 1inch.

**Stablecoins and Wrapped Tokens.** After analyzing the transaction logs and account state differences, we found that TC withdrawers frequently convert their assets into stablecoins (USDT-22.61%, USDC-12.12%, and DAI-11.12%) and wrapped tokens (WETH-36.03% and WBTC-3.85%) for greater fungibility and cross-chain interoperability. These conversions from highly tainted ETH inputs result in comparably high impurity scores across all tokens. It is worth noting that USDT (Tether [36]) and USDC (Circle Internet Financial [8]) are centrally issued by U.S.-based companies. Their token contracts have explicit blacklist mechanisms, `addBlackList (0x0ecb93c0)` and `blacklist (0xf9f92be4)`, theoretically allowing privileged addresses (0xAC3B...1FA0 and 0x10DF...AD2e) to freeze assets held by sanctioned entities. However, quantitative analysis of our dataset revealed that only 40 addresses holding tainted USDT and only 2 addresses holding tainted USDC experienced asset freezing. Our data also showed no statistically significant difference in token selection patterns between potentially freezable tokens (USDT, USDC) and non-freezable alternatives (WETH, WBTC, DAI). This suggests that the theoretical risk of asset freezing does not substantially influence withdrawers' token selection strategies, highlighting a significant gap between technical capability and operational enforcement.

**Other ERC-20 Tokens.** Our tracking algorithm captures transactions involving 9,488 unique ERC-20 token contracts. Through transaction graph clustering and flow analysis, we identified two distinct patterns associated with prevalent scam methodologies: *(i)* rug pull scams, and *(ii)* address poisoning scams. Appendix D provides the corresponding workflows for both schemes.

*6.2.2 Cross-Chain Bridges.* Cross-chain bridges have emerged as pivotal components within the cryptocurrency ecosystem, enabling users to seamlessly transfer assets and messages across disparate blockchain networks. Although these mechanisms facilitate interoperability and expand use cases, they also pose significant challenges to on-chain forensics and censorship efforts, as shown in Figure 5.

**Plaintext Metadata.** Most cross-chain protocols disclose core transaction parameters in plaintext, including the destination chain identifier and the recipient address on the destination chain. In principle, these metadata enable analyzers to link an outgoing transaction on one chain to its corresponding incoming transaction on another. However, a lack of standardization across bridging protocols, especially when destination chains are non-EVM-compatible, hampers this process. Even identifiers for the same blockchain can vary between services built on top of the same underlying infrastructure. For instance, Stargate: Pool Native uses 0x75e8 (30184) to represent the Base blockchain, while Across Protocol: Ethereum Spoke Pool V2 uses 0x2105 (8453), the former adopting the Endpoint

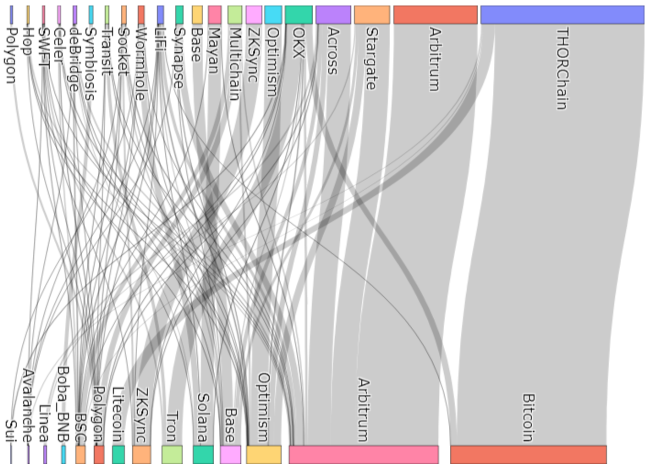

**Figure 5: Flow of Funds via Cross-Chain Bridges. We implement custom parsers for 20 bridges and 2 proxy aggregators to get the corresponding target chain from the transaction metadata. Among over 15 destinations, Bitcoin (33.31%) and EVM-compatible blockchains (53.02%) are primary options.**

ID and the latter using the Chain ID defined by LayerZero[2]. Such inconsistencies necessitate the development of custom parsers for each bridge implementation, significantly increasing the effort required to integrate, interpret, and verify metadata across platforms.

To address this challenge, we developed custom parsers for 20 widely used cross-chain bridges and 2 proxy aggregators (OKX: Web3 Proxy and LI.FI: LiFi Diamond) frequently involved in TC withdrawals. Our analysis revealed that $\mathcal{I}_v = 350,918.15$ ETH ($\varphi \approx 97.37\%$) were bridged out of Ethereum via these platforms, contributing to 32.41% of total impurity volume. EVM-compatible chains accounted for more than half (53.02%) of the bridged impurity volume, including eight Layer-2 rollups and two alternative Layer-1 chains. Among heterogeneous targets, Bitcoin emerged as the dominant destination, capturing 33.31% of bridged volume where 95.95% of them were routed through THORChain. Solana and Litecoin accounted for an additional 4.30% and 2.51%, respectively. However, some bridges such as Chainflip ($\mathcal{I}_v = 4,601.81$ ETH, $\varphi = 97.80\%$) and Orbiter ($\mathcal{I}_v = 1952.27$ ETH, $\varphi = 93.23\%$) do not provide sufficient on-chain information, preventing identification of destination chains or recipient addresses via transaction analysis.

**Transfer Directions.** A common case for cross-chain bridges involves the transfer of assets from Ethereum to Layer-2 solutions (e.g., Arbitrum) or alternative Layer-1 networks (e.g., Bitcoin). In such cases, the user deposits assets into a smart contract on Ethereum, and the bridge protocol either mints or unlocks equivalent assets on the destination chain. Conversely, assets originating on other chains can also be bridged into Ethereum via similar mechanisms. A more complex scenario involves *round-trip* transfers, where assets depart from Ethereum, optionally traverse multiple intermediate chains, and eventually return to Ethereum. Each cross-chain hop fragments the transaction trail, significantly complicating efforts to reconstruct a coherent history of asset movements.

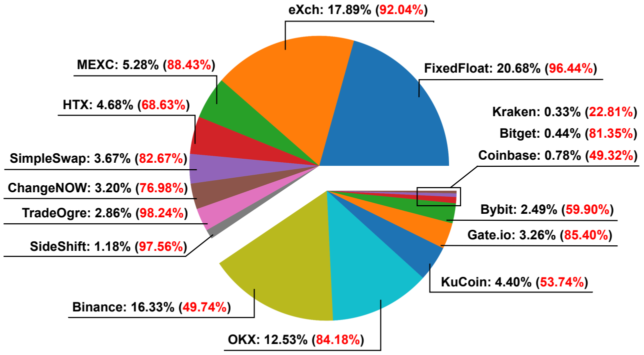

**Figure 6: The distribution of tainted funds deposited into selected CEX, categorized by 8 Non-KYC platforms (up) and 8 KYC-compliant ones (down). The black percentages are proportions of impurity volumes into these platforms, while the red percentages reflect the corresponding impurity scores.**

**Motivations.** *(i) Hard Fork Tolerance*: The DAO hard fork [23] in 2016 highlighted Ethereum's capacity to reverse transactions through community-driven rollbacks. Because this outcome undermined finality for malicious actors, they would bridge funds to different chains, aiming to reduce the likelihood of reversal. *(ii) Heightened Obfuscation:* Each newly designed blockchain or newly developed cross-chain bridge introduces additional complexity into the transaction tracing. This challenge is amplified when intermediary chains provide limited transparency or lack robust blockchain analytics tooling. Moreover, certain blockchains support built-in or composable privacy-enhancing mechanisms (e.g., confidential transactions on Monero, CoinJoin on Bitcoin and TC on Ethereum). Users can strategically route funds through chains with advanced anonymity features to further obscure the provenance of assets. When privacy tools are chained together, e.g., bridging from Ethereum to Bitcoin for CoinJoin, then returning to Ethereum for TC, the difficulty of end-to-end tracing increases exponentially. The limited regulatory or compliance enforcement on newly developed chains (e.g., Boba and Sui) also incentivizes cross-chain transfers for evading detection. *(iii) Lower Fees and Faster Confirmations:* Layer-2 rollups and some Layer-1 blockchains offer significantly reduced transaction costs and faster block finality compared to Ethereum. While these properties benefit users seeking performance and affordability, they are equally attractive to malicious actors seeking to move funds cheaply and efficiently.

### 6.2.3 *Centralized Exchanges.*

CEX serve as significant on- and off-ramps for cryptocurrency markets, bridging the gap between digital and fiat currencies. Their ability to convert large sums of crypto into fiat and vice versa makes them pivotal in AML and CTF processes. Despite the potential exposure to increased surveillance risks, CEX remain a frequent choice (10.37%) among TC withdrawers.

**KYC vs. Non-KYC Compliance.** A CEX that follows KYC compliance typically mandates identity verification procedures, such as submitting government-issued identification, to fulfill regulatory

[2] https://docs.layerzero.network/v2/deployments/deployed-contracts

requirements. Users are generally required to pass these checks to deposit or withdraw fiat currencies, and often when transacting significant volumes of assets. However, in practice, many exchanges, which are nominally KYC-compliant, only require partial identity verification, usually triggered when users interact with fiat gateways. In these cases, users who fail to provide the necessary documentation may face service restrictions or be forced into refund mechanisms, particularly when their behavior raises compliance risks (e.g., as observed on platforms like ChangeNOW [3] and SimpleSwap[4]). To better reflect real-world behavior, we extend the definition of non-KYC-compliant CEX to include those platforms that do not require personal information for account registration and for crypto-to-crypto transactions. In such settings, linkabilities *(i)* between deposit and withdrawal interactions with CEX is broken when analyzing on-chain information, and *(ii)* between CEX's internal accounts and off-chain user identifiers is also broken. As a result, once funds move through these non-KYC-compliant CEX, tracing them becomes highly improbable unless these exchanges record the transaction history and are willing to share them.

**Impurity Volume, Impurity Score and Active Spans.** We analyzed 16 CEX in total, 8 KYC-compliant and 8 non-KYC-compliant, focusing on three key metrics: impurity volume $\mathcal{I}_v$, impurity score $\varphi$, and active spans (the number of days on which deposits with $\varphi > \Phi$ are detected). Figure 6 and Table 6 summarize our findings. Several non-KYC-complaint CEX (e.g., ChangeNOW, FixedFloat, and eXch, highlighted in Table 6) exhibit either a larger number of active days or a higher impurity volume compared to top-tier KYC-compliant CEX (e.g., Coinbase and KuCoin). We also observed higher impurity scores for deposits into non-KYC-compliant CEX relative to their KYC-compliant counterparts. The lack of stringent identity checks reduces the risk of immediate account suspension or asset freezing, making these Non-KYC platforms more attractive.

Notably, U.S.-based platforms (i.e., Coinbase and Kraken) demonstrate relatively low impurity amounts and scores. This pattern is likely attributable to strict regulatory under the OFAC sanctions targeting TC, which encourages stricter transaction screening and discourages high-risk deposits. Conversely, due to the complexity of cross-jurisdictional enforcement, some KYC-complaint CEX based outside the U.S. (e.g., OKX and Bybit) may not follow the specific OFAC sanctions. Therefore, their impurity scores resembled those of non-KYC-compliant platforms, even though their official websites claim compliance with AML and CTF policies.

*6.2.4 Additional Analysis of Service Usages.* Due to the space constraint, detailed analyses of *(i)* privacy-enhancing tools and *(ii)* miscellaneous services have been moved to Appendix E.

## 7 DISCUSSION

We discuss our algorithms through four lenses: scalability, robustness against a real-world exploit, limitations, and ethics.

### 7.1 Scalability

We discuss the scalability of our framework to demonstrate its practical applicability in production environments.

*7.1.1 Extensibility to Target Sources.* While our current implementation utilizes TC as the primary data source, we can create different target sources with the corresponding block numbers for sanctioned entities or security incidents, and can stop updating when some entities are removed from the sanction list. Such extensibility ensures our work maintains relevance as regulatory landscapes evolve. Our framework also accommodates the regulatory diversity inherent in global financial monitoring. Different jurisdictions maintain distinct sanctions lists reflecting their specific regulatory frameworks and national security priorities. A financial institution operating across multiple regions can simultaneously maintain separate sanction profiles for OFAC (US), OFSI (UK), and EU regulatory requirements. This jurisdictional flexibility significantly enhances the system's utility in complex regulatory environments where compliance requirements vary across geographical boundaries.

*7.1.2 Cross-Chain Compatibility.* The fundamental architecture of our scoring algorithm extends beyond Ethereum to encompass all EVM-compatible blockchains utilizing the account model. This cross-chain compatibility is inherent to our design because our impurity scoring system directly aligns with how account-based blockchains update states. Our algorithm leverages this state transition model by propagating impurity scores whenever value transfers occur between accounts. When an account receives funds, our algorithm calculates its new impurity score based on the sender's score and the proportion of value transferred. This calculation maps naturally to the account model's balance updates, which occur at each block as transactions modify account states. This structural alignment means our algorithm can be deployed on any blockchain that follows the same account-state paradigm with minimal adaptation, requiring only configuration changes to interact with different RPC endpoints and chain-specific parameters.

Our tracking implementation includes specialized parsers for 20 popular cross-chain bridges and 2 proxy aggregators capable of extracting destination chain identifiers and recipient addresses from metadata of cross-chain transactions. This capability enables continuous tracking when funds transition between blockchains. By deploying our algorithm on an archive node of the destination chain and adding the corresponding recipient to the target source, we maintain visibility across blockchain boundaries.

*7.1.3 Real-time Performance.* We conducted comprehensive performance measurements under conditions designed to simulate real-world operational demands. Both the Ethereum archive node and our algorithms are deployed on the same hardware platform, with detailed specifications provided in Appendix G. The evaluation methodology of querying operations incorporated *(i)* random selection of 100,000 addresses with impurity amount, *(ii)* generation of 100,000 random addresses without impurity amount, and *(iii)* random selection of 100,000 block numbers for historical queries. It is worth noting that addresses without impurity amount require extra `eth_getBalance` API calls to get their tuple $\langle\, \mathcal{I} = 0,\ \mathcal{B},\ \varphi = 0 \,\rangle$. We also restored the database from random starting points to process 100,000 consecutive blocks for updating operations. Each operation type was executed ten times, with results averaged to ensure statistical validity. Table 3 presents the average execution times for the different types of operations tested.

[3] https://changenow.io/en/terms-of-use/changenow-terms

[4] https://simpleswap.io/terms-of-service

**Table 3: Average Execution Time of Querying and Updating**

| Operation Type | Average Time |
|---|---|
| Query Latest Impurity of Tainted Address (Cached) | 2 ± 1 $\mu s$ |
| Query Latest Impurity of Tainted Address | 74 ± 26 $\mu s$ |
| Query Latest Impurity of Untainted Address | 225 ± 29 $\mu s$ |
| Query Historical Impurity of Tainted Address | 358 ± 72 $\mu s$ |
| Query Historical Impurity of Untainted Address | 372 ± 49 $\mu s$ |
| Update Impurity for New Block | 0.07 ± 0.03 $s$ |

Our database architecture maintains separate tables for different query types, optimizing both latest-state queries and historical-state lookups. This design choice enables the system to efficiently handle both real-time monitoring (requiring the latest state) and forensic analysis (requiring historical state reconstruction) without performance compromises. Moreover, we use MDBX database engine, which is a high-performance key-value store that utilizes memory-mapped file technology, which significantly enhances query performance for blockchain analysis applications. This caching mechanisms in MDBX is effective because addresses with impurity amount frequently appear in multiple transactions, creating natural temporal locality that caching exploits.

The performance results demonstrate that all querying operations complete in under 500 $\mu s$. Notably, cached impurity score queries execute in as little as 1 $\mu s$. The algorithm demonstrates the capability to update impurity scores at a rate exceeding 10 blocks per second, which translates to processing more than 1,500 transactions per second (TPS). As shown in Table 7, this processing capacity significantly exceeds the throughput of major EVM-compatible blockchain networks, including Ethereum, BNB, and prominent Layer-2 solutions. The performance characteristics demonstrated by our implementation make it suitable for integration into existing blockchain monitoring infrastructure without introducing computational bottlenecks. This efficiency is critical for applications requiring real-time compliance monitoring and timely identification of potentially malicious activities.

## 7.2 Robustness

To our knowledge, this paper presents the first comprehensive analysis of sanctioned addresses on Ethereum, specifically for TC withdrawers. To evaluate the robustness and scalability of our algorithms, we applied them to the Bybit exploit (the largest known security incident [13] in history until March 2025).

*7.2.1 Proxy Ground Truth and Evaluation Results.* By the end of our study period (March 21, 2025), we found only two public datasets that contained Ethereum addresses involved in the Bybit exploit: *(i)* 71 addresses from Etherscan's Label Cloud API [15], and *(ii)* 12,394 addresses from Elliptic's Exploit API [12]. Specifically, Etherscan assigned addresses a label of "Bybit Exploiter" on its website. Elliptic added and removed addresses based on their own proprietary risk assessment methodology, to which we had no access. Because the Etherscan dataset is a subset of the Elliptic dataset, we consequently built a ground truth with 12,394 addresses. We include a backup of both the Etherscan and Elliptic datasets in our public repository.

Figure 9 in Appendix A illustrates the relationship between varying threshold values and the corresponding precision and recall metrics when applied to our algorithms. There is significant decline in precision from approximately 97% to 67% (and lower) at thresholds $\Phi \leq 2.6\%$. Conversely, recall demonstrates remarkable stability (around 75%) across the threshold spectrum. We emphasize that this result is context-dependent and may not generalize across all malicious activity detection scenarios. Regulatory bodies prioritizing minimization of false positives might opt for higher thresholds, whereas those emphasizing comprehensive detection of malicious activities might select lower thresholds while accepting increased verification overhead. Here we use a conservative threshold (set $\Phi = 5\%$) to reduce the false positives. As shown in Table 4, we compared addresses collected by our algorithms under this threshold with the proxy ground truth.

**Table 4: Evaluation Algorithms on Proxy Ground Truth**

| | Ground Truth | Our Algorithms † | | | | | |
|---|---|---|---|---|---|---|---|
| | | TP | TN | FP ‡ | FN | Precision ‡ | Recall |
| # Address | 12,210 | 9,045 | / | 221 | 3,165 | 97.61% | 74.08% |

† The performance of our algorithms is based on the selection of scoring threshold.

‡ 118 false positives are service providers and the remaining 103 addresses are novel discoveries not included in the ground truth, such that our precision can reach 100%.

*7.2.2 Precision and Result Validity.* Our algorithm flagged totally 9,266 addresses and 9,045 of them existed in the ground truth dataset (precision ≈ 97.61%). Analysis of the 221 apparent false positives revealed two distinct categories: *(i)* 118 addresses (53.39%) corresponded to general-purpose services (e.g., DEX or cross-chain bridges) utilized by attackers. While not inherently malicious, we included these addresses in our algorithm and aimed to provide quantitative insights for these service providers; and *(ii)* the remaining 103 addresses (46.61%) were novel discoveries not included in the ground truth. Through manual verifications, we confirmed these addresses' participation in the attack sequence. This finding indicated potential completeness limitations in existing public datasets when documenting complex attacks. After considering these results, the adjusted precision reaches 100%.

We further randomly checked false positives that appeared when threshold $\Phi \leq 2.6\%$ and found that *(i)* there were more addresses controlled by attackers but they were not included in the ground truth dataset; and *(ii)* several addresses were included when the tainted funds flowed into a *super-account* and made this account exceed the threshold. We could not find a corresponding label to determine whether this *super-account* and subsequent addresses were also controlled by attackers. Continually updating the label library can mitigate this problem and improve the precision.

*7.2.3 Recall and Coverage Limitation.* Our analysis revealed that 3,165 addresses in the ground truth were missed (recall ≈ 74.08%), highlighting specific constraints in our approach. Two primary factors affected recall: *(i)* the conservative impurity threshold $\Phi$ introduced false negatives; and *(ii)* our implementation focused on native ETH rather than ERC-20 token transfers. This limitation created a vulnerability to balance manipulation evasion techniques, where adversaries could temporarily drain an address's ETH balance (e.g., flash loans through DEX interactions), mix the ETH with a large liquidity pool, and then swap back to ETH, artificially decreasing the impurity score. Despite these constraints, our method accurately identified the specific ERC-20 tokens exchanged during evasion attempts and quantified their transaction volumes. The algorithm also successfully tracked addresses that use high-impurity ETH as transaction fees for token transfers. However, our algorithms could not identify addresses that successfully perform the balance manipulation and also their derived addresses. In future work, we will extend our approach to include comprehensive ERC-20 token tracking and eventually enhance recall.

### 7.3 Limitations

We acknowledge several limitations in this paper. **Soundness:** The performance of our algorithms depends on the selected threshold. This selection influences the balance between false positives and coverage - a common trade-off in detection systems. We derived this threshold by analyzing results from the Bybit exploit (validated using proxy ground-truth datasets) in conjunction with the global distribution of scores. However, due to the absence of definitive ground truth for addresses involved in sanction evasions, we cannot guarantee that the chosen threshold is optimal. Additionally, the public datasets for the Bybit exploit and the label library for services may introduce unknown biases, as the methods for their data collection are not explicitly documented. We have mitigated this risk by utilizing multiple independent data sources and conducting manual validation. **Completeness:** Our tracking implementation monitors funds until they reach identifiable services. Due to the diversity of Ethereum ecosystem and time constraints, we prioritized analyzing major services identified based on their impurity volume, ultimately accounting for 83.34% of funds withdrawn from TC. Moreover, as shown in Section 7.2.3, our algorithm remains vulnerable to balance manipulation techniques, such as swapping ETH into ERC-20 tokens and subsequently reverting them back to ETH. Hence, our analysis did not represent the full spectrum of evasion techniques. Nevertheless, our work still spotlighted the ineffectiveness of current sanctions. **Implementation Barriers:** We demonstrated the scalability of our algorithms that can be used for cross-chain tracking. However, this capability is built on custom parsers for each bridge protocol. This introduces significant maintenance overhead as existing protocols evolve and new protocols emerge. Moreover, we did not run our algorithms on other EVM-compatible chains. Instead, we compared our algorithm's block-update times against typical block-production intervals of these chains. The observed performance of our algorithms indicates computational margin for incorporating additional complexity.

### 7.4 Ethical Considerations

Sanction enforcement on blockchains is inherently a *Cat-and-Mouse* game. As regulators develop detection and enforcement mechanisms, malicious actors continuously adapt with increasingly sophisticated bypassing strategies. Our research sheds light on this dynamic by revealing the limitations of current sanction approaches, alongside behavior patterns and service dependencies exploited during evasion attempts. To ensure ethical integrity, we restrict our analysis of TC withdrawals to the officially sanctioned period, thereby avoiding scrutiny of users after regulatory exemptions were applied. All data are obtained from publicly available blockchain ledgers, and no personally off-chain identifiable information is used. Although our findings could theoretically be misused, we carefully calibrated our disclosures to support scientific validation and policy analysis while not revealing actionable specifics for circumvention. Our quantitative results highlight behavioral regularities persistent across evasion strategies, contributing to more adaptive and effective compliance mechanisms. Additionally, our work supports regulators and service providers in developing oversight frameworks capable of evolving alongside evasion techniques while minimizing the impact on legitimate users.

## 8 RELATED WORK

Our work builds upon previous research on blockchain transaction analysis and privacy mechanisms. Prior works by Wu et al. [46] and Gomez et al. [17] established graph-based approaches for tracking malicious funds from security incidents, while Lin et al. [21] proposed density-based detection of money laundering patterns on Ethereum. Anonymity analyses in [11, 19, 42, 43] evaluated the capability of privacy-enhancing protocols using heuristic-based or machine-learning-based approaches. Yousaf et al. [47] first identified the complexity of cross-chain tracing between blockchains that have anonymous mechanism, while our research implements custom parsers for major bridge protocols.

Zola et al. [51] first showed the ineffectiveness of sanctions on Bitcoin, but limited their analysis at 2-step transaction graphs. Möser et al. [24] also proposed a risk scoring mechanism on Bitcoin. However, the account model of Ethereum and the capability of smart contracts bring more mechanisms for both censorship and obfuscation. Wahrstätter et al. [40] documented censorship at the block production level, measuring validator compliance with OFAC sanctions, but lacked quantitative metrics for downstream fund propagation. Our work provides the first comprehensive empirical analysis of sanction effectiveness on Ethereum, introducing a quantitative framework that evaluates both direct compliance and subsequent circumvention patterns with high precision. Moreover, our implementation can be extended to EVM-compatible chains with real-time performance, enabling cross-chain tracking.

## 9 CONCLUSION

This paper presents the first quantitative evaluation of blockchain sanctions effectiveness. We use TC as a case study, analyzing 957 days of Ethereum data. We demonstrate the inherent limitations of binary classification approaches for distinguishing malicious transactions, evidenced by dusting attacks, and introduce a impurity metric achieving 97.61% precision and 74.08% recall in tracking malicious funds. Our findings reveal that while general TC deposit volume decreased by 71.03% post-sanctions, malicious actors continued exploiting TC in 78.33% of security incidents. This continued exploitation is facilitated by inconsistent validator-level enforcement and sophisticated evasion techniques including specific behavior patterns and strategic service selection. These insights provide concrete recommendations for regulatory authorities and compliance teams, helping them balance privacy concerns with financial oversight requirements using quantitative risk frameworks.

## REFERENCES

[1] 1inch Network. 2025. 1inch Protocol. https://1inch.io/ Accessed: 2025-04-10.
[2] Aave. 2025. Aave: Open Source Liquidity Protocol. https://aave.com/ Accessed: 2025-04-10.

[3] Andre Augusto, Rafael Belchior, Miguel Correia, Andre Vasconcelos, Luyao Zhang, and Thomas Hardjono. 2024. SoK: Security and Privacy of Blockchain Interoperability . In *2024 IEEE Symposium on Security and Privacy (SP)*. IEEE Computer Society, Los Alamitos, CA, USA, 3840–3865. doi:10.1109/SP54263.2024.00255

[4] Christian Badertscher, Mahdi Sedaghat, and Hendrik Waldner. 2023. Unlinkable Policy-Compliant Signatures for Compliant and Decentralized Anonymous Payments. Cryptology ePrint Archive, Paper 2023/1070. https://eprint.iacr.org/2023/1070

[5] Austin R. Benson, David F. Gleich, and Jure Leskovec. 2016. Higher-order organization of complex networks. *Science* 353, 6295 (2016), 163–166. doi:10.1126/science.aad9029 arXiv:https://www.science.org/doi/pdf/10.1126/science.aad9029

[6] Binance. 2025. Binance Exchange. https://www.binance.com/ Accessed: 2025-04-10.

[7] Chainalysis. 2022. Free Cryptocurrency Sanctions Screening Tools. https://www.chainalysis.com/free-cryptocurrency-sanctions-screening-tools/ Accessed: 2025-04-10.

[8] Circle Internet Financial. 2025. Circle: USDC & Developer Services for a New Financial System. https://www.circle.com/ Accessed: 2025-04-10.

[9] Coinbase. 2025. Coinbase Exchange. https://www.coinbase.com/ Accessed: 2025-04-10.

[10] Compound Finance. 2025. Compound Finance: Decentralized Interest Rate Protocol. https://compound.finance/ Accessed: 2025-04-10.

[11] Hanbiao Du, Zheng Che, Meng Shen, Liehuang Zhu, and Jiankun Hu. 2024. Breaking the Anonymity of Ethereum Mixing Services Using Graph Feature Learning. *IEEE Transactions on Information Forensics and Security* 19 (2024), 616–631. doi:10.1109/TIFS.2023.3326984

[12] Elliptic. 2025. Bybit Exploit Blocklist. https://www.elliptic.co/bybit-exploit-blocklist Accessed: 2025-04-10.

[13] Elliptic. 2025. The largest theft in history - following the money trail from the Bybit Hack. https://www.elliptic.co/blog/bybit-hack-largest-in-history Accessed: 2025-04-10.

[14] Ethereum Foundation. 2024. ERC-20 Token Standard. https://ethereum.org/en/developers/docs/standards/tokens/erc-20/ Accessed: 2025-04-10.

[15] Etherscan. 2025. Ethereum Accounts Labeled 'Bybit Exploit'. https://etherscan.io/accounts/label/bybit-exploit Accessed: 2025-04-10.

[16] Financial Action Task Force. 2023. Virtual Assets: Targeted Update on Implementation of the FATF Standards on Virtual Assets and Virtual Asset Service Providers. https://www.fatf-gafi.org/en/publications/Fatfrecommendations/targeted-update-virtual-assets-vasps-2023.html Accessed: 2025-04-10.

[17] Gibran Gomez, Pedro Moreno-Sanchez, and Juan Caballero. 2022. Watch Your Back: Identifying Cybercrime Financial Relationships in Bitcoin through Back-and-Forth Exploration. In *Proceedings of the 2022 ACM SIGSAC Conference on Computer and Communications Security* (Los Angeles, CA, USA) *(CCS '22)*. Association for Computing Machinery, New York, NY, USA, 1291–1305. doi:10.1145/3548606.3560587

[18] Shixuan Guan and Kai Li. 2024. Characterizing Ethereum Address Poisoning Attack. In *Proceedings of the 2024 on ACM SIGSAC Conference on Computer and Communications Security* (Salt Lake City, UT, USA) *(CCS '24)*. Association for Computing Machinery, New York, NY, USA, 986–1000. doi:10.1145/3658644.3690277

[19] Alex Márk Kovács and István András Seres. 2024. Anonymity Analysis of the Umbra Stealth Address Scheme on Ethereum. In *Companion Proceedings of the ACM Web Conference 2024* (Singapore, Singapore) *(WWW '24)*. Association for Computing Machinery, New York, NY, USA, 1768–1775. doi:10.1145/3589335.3651963

[20] Ya-Nan Li, Tian Qiu, and Qiang Tang. 2023. Pisces: Private and Compliable Cryptocurrency Exchange. *arXiv preprint arXiv:2309.01667* (2023).

[21] Dan Lin, Jiajing Wu, Yunmei Yu, Qishuang Fu, Zibin Zheng, and Changlin Yang. 2024. DenseFlow: Spotting Cryptocurrency Money Laundering in Ethereum Transaction Graphs. In *Proceedings of the ACM Web Conference 2024* (Singapore, Singapore) *(WWW '24)*. Association for Computing Machinery, New York, NY, USA, 4429–4438. doi:10.1145/3589334.3645692

[22] Gregory Maxwell. 2013. CoinJoin: Bitcoin privacy for the real world. https://bitcointalk.org/?topic=279249 Accessed: 2025-04-10.

[23] Muhammad Izhar Mehar, Charles Louis Shier, Alana Giambattista, Elgar Gong, Gabrielle Fletcher, Ryan Sanayhie, Henry M Kim, and Marek Laskowski. 2019. Understanding a revolutionary and flawed grand experiment in blockchain: the DAO attack. *Journal of Cases on Information Technology (JCIT)* 21, 1 (2019), 19–32.

[24] Malte Möser, Rainer Böhme, and Dominic Breuker. 2014. Towards Risk Scoring of Bitcoin Transactions. In *Financial Cryptography and Data Security*, Rainer Böhme, Michael Brenner, Tyler Moore, and Matthew Smith (Eds.). Springer Berlin Heidelberg, Berlin, Heidelberg, 16–32.

[25] Satoshi Nakamoto. 2008. Bitcoin: A peer-to-peer electronic cash system. *Decentralized business review* (2008).

[26] Aztec Network. 2023. Sunsetting Aztec Connect. https://aztec.network/blog/sunsetting-aztec-connect Accessed: 2025-04-10.

[27] Rekt News. 2022. Nomad Bridge - Rekt. https://rekt.news/nomad-rekt/. Accessed: 2025-04-10.

[28] Rekt News. 2023. HECO Bridge - Rekt. https://rekt.news/heco-htx-rekt/. Accessed: 2025-04-10.

[29] Rekt News. 2024. Orbit Bridge - Rekt. https://rekt.news/orbit-bridge-rekt/. Accessed: 2025-04-10.

[30] Nocturne. 2023. Nocturne Documentation. https://nocturne-xyz.gitbook.io/nocturne Accessed: 2025-04-10.

[31] Vladimir Popov, Mikhail Krupin, Andrew Gross, and Georgi Koreli. 2024. Blockchain Privacy and Self-regulatory Compliance: Methods and Applications. *Available at SSRN 4787693* (2024).

[32] Kaihua Qin, Liyi Zhou, and Arthur Gervais. 2022. Quantifying Blockchain Extractable Value: How dark is the forest?. In *2022 IEEE Symposium on Security and Privacy (SP)*. 198–214. doi:10.1109/SP46214.2022.9833734

[33] RAILGUN Project. 2025. RAILGUN Wiki. https://docs.railgun.org/wiki Accessed: 2025-04-10.

[34] ScopeLift. 2025. Umbra: Privacy-Preserving Stealth Payments. https://app.umbra.cash/ Accessed: 2025-04-10.

[35] Secret Network. 2024. Secret Tunnel. https://tunnel.scrt.network/ Accessed: 2025-04-10.

[36] Tether Operations Limited. 2025. Tether: Digital Tokens Backed by Real-World Assets. https://tether.to/ Accessed: 2025-04-10.

[37] Uniswap Labs. 2025. Uniswap Procotol. https://app.uniswap.org/ Accessed: 2025-04-10.

[38] U.S. Department of the Treasury. 2022. U.S. Treasury Sanctions Notorious Virtual Currency Mixer Tornado Cash. https://home.treasury.gov/news/press-releases/jy0916 Accessed: 2025-04-10.

[39] U.S. Department of the Treasury. 2025. Tornado Cash Delisting. https://home.treasury.gov/news/press-releases/sb0057 Accessed: 2025-04-10.

[40] Anton Wahrstätter, Jens Ernstberger, Aviv Yaish, Liyi Zhou, Kaihua Qin, Taro Tsuchiya, Sebastian Steinhorst, Davor Svetinovic, Nicolas Christin, Mikolaj Barczentewicz, and Arthur Gervais. 2024. Blockchain Censorship. In *Proceedings of the ACM Web Conference 2024* (Singapore, Singapore) *(WWW '24)*. Association for Computing Machinery, New York, NY, USA, 1632–1643. doi:10.1145/3589334.3645431

[41] Anton Wahrstatter, Jorao Gomes, Sajjad Khan, and Davor Svetinovic. 2023. Improving Cryptocurrency Crime Detection: CoinJoin Community Detection Approach . *IEEE Transactions on Dependable and Secure Computing* 20, 06 (Nov. 2023), 4946–4956. doi:10.1109/TDSC.2023.3238412

[42] Anton Wahrstatter, Alfred Taudes, and Davor Svetinovic. 2024. Reducing Privacy of CoinJoin Transactions: Quantitative Bitcoin Network Analysis . *IEEE Transactions on Dependable and Secure Computing* 21, 05 (Sept. 2024), 4543–4558. doi:10.1109/TDSC.2024.3353803

[43] Zhipeng Wang, Stefanos Chaliasos, Kaihua Qin, Liyi Zhou, Lifeng Gao, Pascal Berrang, Benjamin Livshits, and Arthur Gervais. 2023. On How Zero-Knowledge Proof Blockchain Mixers Improve, and Worsen User Privacy. In *Proceedings of the ACM Web Conference 2023* (Austin, TX, USA) *(WWW '23)*. Association for Computing Machinery, New York, NY, USA, 2022–2032. doi:10.1145/3543507.3583217

[44] Sam Werner, Daniel Perez, Lewis Gudgeon, Ariah Klages-Mundt, Dominik Harz, and William Knottenbelt. 2023. SoK: Decentralized Finance (DeFi). In *Proceedings of the 4th ACM Conference on Advances in Financial Technologies* (Cambridge, MA, USA) *(AFT '22)*. Association for Computing Machinery, New York, NY, USA, 30–46. doi:10.1145/3558535.3559780

[45] Gavin Wood et al. 2014. Ethereum: A secure decentralised generalised transaction ledger. *Ethereum project yellow paper* 151, 2014 (2014), 1–32.

[46] Jiajing Wu, Dan Lin, Qishuang Fu, Shuo Yang, Ting Chen, Zibin Zheng, and Bowen Song. 2024. Toward Understanding Asset Flows in Crypto Money Laundering Through the Lenses of Ethereum Heists. *IEEE Transactions on Information Forensics and Security* 19 (2024), 1994–2009. doi:10.1109/TIFS.2023.3346276

[47] Haaroon Yousaf, George Kappos, and Sarah Meiklejohn. 2019. Tracing Transactions Across Cryptocurrency Ledgers. In *28th USENIX Security Symposium (USENIX Security 19)*. USENIX Association, Santa Clara, CA, 837–850. https://www.usenix.org/conference/usenixsecurity19/presentation/yousaf

[48] Zhao Zhang, Chunxiang Xu, and Yunxia Han. 2024. Privacy-Preserving Cryptocurrency With Threshold Authentication and Regulation. *IEEE Transactions on Information Forensics and Security* 19 (2024), 6620–6635. doi:10.1109/TIFS.2024.3419694

[49] Liyi Zhou, Xihan Xiong, Jens Ernstberger, Stefanos Chaliasos, Zhipeng Wang, Ye Wang, Kaihua Qin, Roger Wattenhofer, Dawn Song, and Arthur Gervais. 2023. SoK: Decentralized Finance (DeFi) Attacks . In *2023 IEEE Symposium on Security and Privacy (SP)*. IEEE Computer Society, Los Alamitos, CA, USA, 2444–2461. doi:10.1109/SP46215.2023.10179435

[50] zkBob. 2025. zkBob: Your Web3 Wallet With Privacy Option! https://www.zkbob.com/ Accessed: 2025-04-10.

[51] Francesco Zola, Jon Ander Medina, and Raul Orduna. 2024. Assessing the Impact of Sanctions in the Crypto Ecosystem: Effective Measures or Ineffective Deterrents? arXiv:2409.10031 [cs.CR] https://arxiv.org/abs/2409.10031

# A CASE STUDY: BYBIT EXPLOIT

We applied our impurity-based tracking algorithm to the Bybit exploit in order to validate its effectiveness. Figure 7 shows the complexity of transaction graph, illustrating the sophisticated multi-stage fund dispersal and obfuscation techniques. Figure 8 further demonstrates that the exploiter exhibits similar transaction motifs to TC withdrawers. Specifically, intense activity in asset transfer (012C), splitting (021D), and merging (021U) patterns. Figure 9 presents the performance across impurity thresholds $\Phi$. Precision remains above 97% for thresholds $\Phi > 2.6\%$, while recall stays stable. We choose a conservative threshold $\Phi = 5\%$ to reduce false positives without significantly compromising detection coverage.

# B ALGORITHM

In this section, we provide the algorithm for updating the impurity score of each affected address as sanctioned assets propagate.

**Algorithm 1:** Impurity Updating Algorithm

```
Data: Blockchain states $\{(s_0, s_1, \ldots, s_{n-1}) \mid s \in \mathcal{S}\}$, Valid
      Ethereum address set $ADDR$, Sanctioned address set
      $ADDR_{sanction} \subset ADDR$, First state after sanctions $s_{OFAC}$
Result: Historical records of for $\langle \mathcal{I}, \mathcal{B}, \varphi \rangle$ all involved addresses at
        each state $s$ where $\mathcal{I}$ is the impurity amount, $\mathcal{B}$ is the
        balance amount, and $\varphi$ is the impurity score (cf. Section 4.1)
Initialization:
$s_0 = s_{OFAC}$;
for each address $addr \in ADDR_{sanction}$ do
    Set $\mathcal{I}(s_{OFAC}, addr) = \mathcal{B}(s_{OFAC}, addr)$;
end
for each address $addr \notin ADDR_{sanction}$ do
    Set $\mathcal{I}(s_{OFAC}, addr) = 0$;
end
State Transition and Attribute Update:
for $i \in [0, n-1)$ do
    Let balance state transition $\mathcal{T}_{\mathcal{B}}(s_i, op_{\mathcal{B}}) \rightarrow s_{i+1}$ where affected
      addresses and amounts are extracted from the operation $op_{\mathcal{B}}$:
    $op_{\mathcal{B}} \rightarrow \{\langle addr_{from}, a_{sent} \rangle, \langle addr_{to}, a_{received} \rangle\}$;
    Update:
    $\mathcal{I}(s_{i+1}, addr_{from}) = \mathcal{I}(s_i, addr_{from}) - \left\lceil \frac{a_{sent} \cdot \mathcal{I}(s_i, addr_{from})}{\mathcal{B}(s_i, addr_{from})} \right\rceil$;
    if address $addr_{to} \in ADDR_{Sanction}$ then
        $\mathcal{I}(s_{i+1}, addr_{to}) = \mathcal{B}(s_{i+1}, addr_{to})$;
    else
        $\mathcal{I}(s_{i+1}, addr_{to}) = \mathcal{I}(s_i, addr_{to}) + \left\lceil \frac{a_{received} \cdot \mathcal{I}(s_i, addr_{from})}{\mathcal{B}(s_i, addr_{from})} \right\rceil$;
    end
    for each address $addr \in \{addr_{from}, addr_{to}\}$ do
        if $\mathcal{B}(s_{i+1}, addr) \neq 0$ then
            $\varphi(s_{i+1}, addr) = \frac{\mathcal{I}(s_{i+1}, addr)}{\mathcal{B}(s_{i+1}, addr)}$;
        else
            $\varphi(s_{i+1}, addr) = 0$;
        end
        Store $\left\langle \mathcal{I}(s_{i+1}, addr), \mathcal{B}(s_{i+1}, addr), \varphi(s_{i+1}, addr) \right\rangle$
    end
end
```

# C IMPOSSIBILITY OF BINARY CLASSIFICATION MECHANISM

We provide an informal argument demonstrating why naïve binary classification system inevitably fails when faced with dusting attacks, thereby necessitating the continuous, quantitative impurity metrics described in Section 4.2. We also discuss the effectiveness of other classification mechanisms in this section.

Let *ADDR* be the set of all valid addresses on the blockchain, and define a general binary classification function:

$$C : ADDR \rightarrow \{0, 1\} \tag{1}$$

where $C(addr) = 0$ means address *addr* is "clean" and $C(addr) = 1$ means *addr* is "tainted." Initially, sanctioned addresses are tainted: $C(addr) = 1$ if $addr \in ADDR_{sanction}$, otherwise $C(addr) = 0$.

For a binary classification system to be useful in blockchain analysis, it must satisfy two key properties:

(1) **Propagation Property**: There must exist some mechanism by which taint propagates from sanctioned addresses to their transaction partners. Without this property, the classification would fail to identify entities interacting with sanctioned addresses.
(2) **Decidability Property**: The classification must be computationally decidable in reasonable time, meaning there exists an efficient algorithm to determine whether an address is tainted.

Any binary classification system satisfying these minimal properties must implement some form of propagation rule. While the specific rule may vary, it must establish conditions under which an address receiving funds from a tainted address also becomes tainted. We denote this general propagation condition:

$$\mathcal{P}(s, addr_{from}, addr_{to}, v) \tag{2}$$

which evaluates to true when a transaction from $addr_{from}$ to $addr_{to}$ with a value $v$ at the blockchain state $s$ causes taint to propagate.

A dusting attack occurs when an attacker controlling a tainted address $addr_s$ (where $C(addr_s) = 1$) creates transactions

$$tx_i : addr_s \rightarrow addr_i \implies \mathcal{P}(s, addr_s, addr_i, v_i) = True \tag{3}$$

with values $v_i$ deliberately chosen to ensure taint is propagated for many strategically selected target addresses $addr_i$. Let $G(s) \subseteq ADDR$ be the set of all tainted addresses at blockchain state $s$, with $G(s_{OFAC}) = ADDR_{sanctioned}$ initially. After each dusting attack, $G(s')$ expands to include the targeted addresses.

The fundamental limitation of naïve binary classification system is that it cannot distinguish between significant and trivial taint exposure: an address is either tainted or not. This creates a vulnerability that can be exploited through strategic dusting: a small-value dusting transaction can instantly taint high-value addresses, creating an amplification effect. From our empirical data in Section 5.1, just 12.00 ETH in dusting transactions tainted over 9,034,251.58 ETH, an amplification factor exceeding 750,000×.

We denote the total value (balance amount) held by tainted addresses flagged by naïve binary classification mechanism as

$$V_{\text{tainted}}(s) = \sum_{addr \in G(s)} \mathcal{B}(s, addr) \tag{4}$$

and denote the total value held by entire addresses as

$$V_{\text{entire}}(s) = \sum_{addr \in ADDR} \mathcal{B}(s, addr) \tag{5}$$

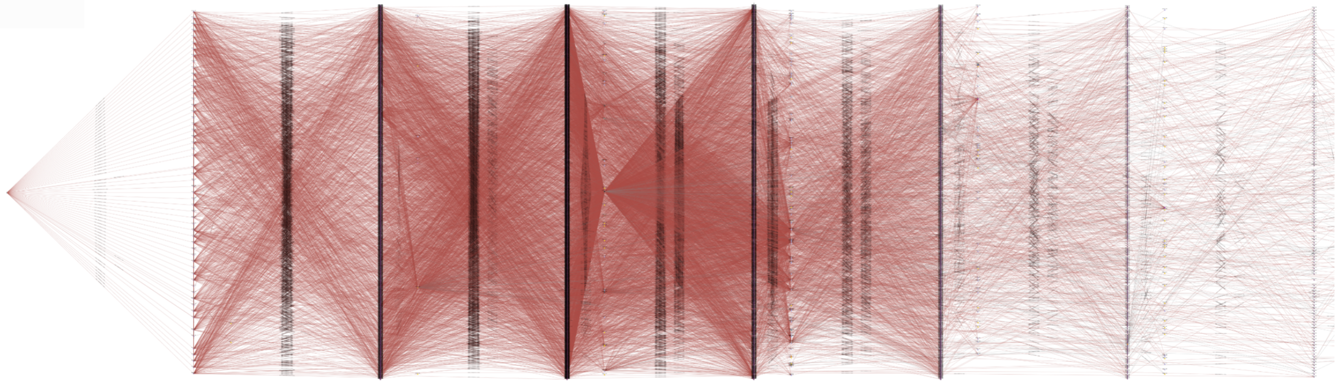

**Figure 7: Visualization of Transaction Flow Patterns in the Bybit Exploit. This figure illustrates sophisticated, multi-stage fund dispersal and obfuscation techniques, wherein stolen assets were distributed through a hierarchical network structure.**

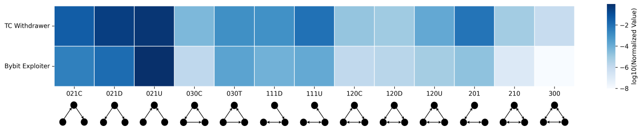

**Figure 8: Heatmap comparing transaction patterns between TC withdrawers and the Bybit exploiter based on connected three-node motifs. Dark blue cells of both distributions in 012C, 021D, and 021U show high-intensity activities of asset transferring, splitting, and merging, respectively.**

Under propagation rules satisfying the minimal properties, strategic dusting attacks to naïve binary classification system can drive

$$\begin{aligned} \lim_{s \to \infty} \frac{|G(s)|}{|ADDR|} &\to 1 \\ \lim_{s \to \infty} V_{\text{tainted}}(s) &\to V_{\text{entire}}(s) \end{aligned} \tag{6}$$

When most addresses become tainted, the system cannot distinguish genuine risk from dust-induced taint, rendering the classification meaningless. Services implementing naïve binary classification face an inevitable denial-of-service vulnerability: either block all tainted addresses (causing service failure as $|G(s)|$ grows) or ignore the classification (rendering it useless). This fundamental limitation was observed with services like Aave Front-End.

The failure of naïve binary classification system directly necessitates a continuous metric such as our impurity score $\varphi(s, addr) \in [0, 1]$. Under dusting attacks, naïve binary classification marks all recipients as completely tainted, while with our continuous metric, $\varphi(s, addr_i) = \frac{\mathcal{I}(s,addr_i)}{\mathcal{B}(s,addr_i)} \approx 0$ for addresses with large balances receiving small dust amounts. This allows the system to distinguish between seriously tainted addresses and those with negligible exposure, preserving the utility of the classification system against dusting attacks. Our impurity updating algorithm in Section 4.2 implements precisely this approach.

In the following of this section, we will discuss the effectiveness of other classification rules from aspect of attackers and evaders:

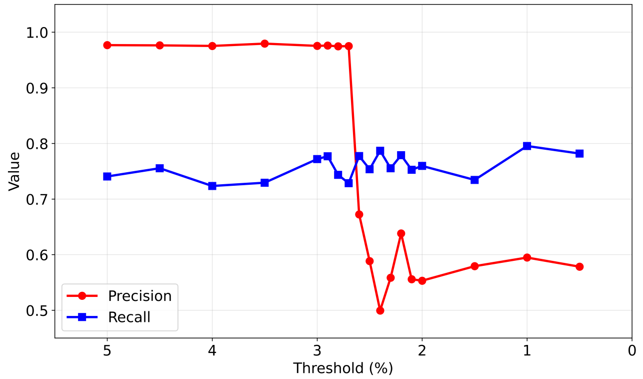

**Figure 9: Performance trade-off with varying impurity thresholds $\Phi$ between 5% and 0.5%. Precision remains high ($>$ 97%) before dropping significantly at thresholds $\Phi \leq 2.6\%$, while recall remains stable across the entire range. This supports our conservative selection of $\Phi = 5\%$ to maximize precision while maintaining acceptable recall.**

(1) **For Time-Based Rules** (e.g., taint expires after time $t$): *(i)* Attackers can refresh the dusting attack periodically; *(ii)* Evaders can bypass the detection via a waiting time longer than $t$.
(2) **For Hop-Based Rules** (e.g., taint if receiving from any address that is within $h$ hops of tainted addresses): *(i)* Attackers can directly issue transactions from tainted addresses to target addresses in 1 hop; *(ii)* Evaders cannot bypass unless they can move assets through addresses or services that reset or do not share the hop count and eventually exceed the hop limit $h$.
(3) **For Value-Threshold Rules** (e.g., taint if receiving more than $\theta$ value from sanctioned addresses):
   - *If the detection only check the value in target addresses: (i)* Attackers can simply send $v > \theta$ in one transaction or analyze on-chain data to send more precision value; *(ii)* Evaders cannot bypass unless they send the amount exceeding $\theta$ to a designated burnt address or divide their balance through services do not apply this detection mechanism.

- *If the detection also check the value in transactions: (i)* Attackers can divide $v > \theta$ into several transactions and send them sequently; *(ii)* Evaders' operations do not change.
- *If the detection even check the value in source addresses: (i)* Attackers can prepare several addresses totally holding $v > \theta$; *(ii)* Evaders' operations do not change.

(4) **For Percentage-Threshold Rules** (e.g., taint if receiving more than $\theta$% of balance from sanctioned addresses):

- *If the detection only check the percentage in target addresses: (i)* Attackers can simply send $v > \theta\% \times \mathcal{B}(s, addr_i)$ in one transaction or analyze on-chain data to send more precision value; *(ii)* Evaders can supply their account with enough "clean" amount to decrease the percentage $\varphi < \theta\%$. This can be done by direct transfer or using balance manipulation (e.g., addresses can drain and restore their balance using services do not apply this detection mechanism, for example, flash loans via DEX and coin mixing via privacy tools).
- *If the detection also check the percentage in transactions: (i)* Attackers can prepare one or more accounts where each account is under the threshold $\varphi < \theta\%$ and collectively send $v > \theta\% \times \mathcal{B}(s, addr_i)$; *(ii)* Evaders' operations do not change.
- *If the detection even check the percentage in source addresses:* Both attackers' and evaders operations do not change.

## D WORKFLOW OF TOKEN SCAMS

**Crafted Tokens for Rug Pull Scams.** Scammers can create ERC-20 tokens and trade these tokens on DEX such as Uniswap to perform rug pull attacks. The process in Figure 10 unfolds:

(1) *Initial TC Withdrawals.* Accounts withdraw ETH from TC.

(2) *ETH Redistribution.* One TC withdrawer consolidates ETH and transfers it to a "token creator" account. Concurrently, other withdrawers distribute ETH to intermediate accounts using automated tools (e.g., multi-sending or batch contracts).

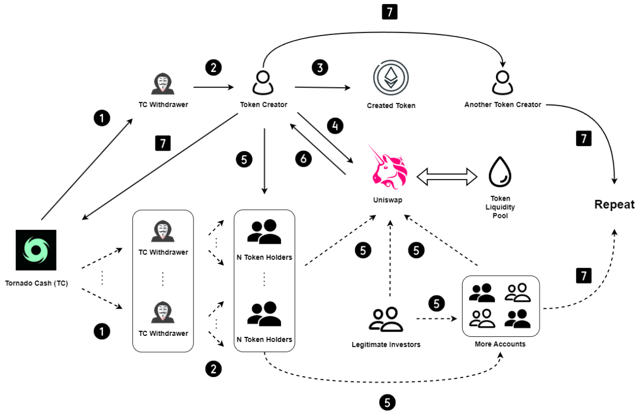

**Figure 10: Crafted Tokens for Rug Pull Scams. The solid lines represent the actions that the token creator will take, and the dashed lines denote how other accounts participant. The workflow includes following steps: ❶ Initial TC Withdrawals, ❷ ETH Redistribution, ❸ Token Deployment, ❹ Liquidity Supplement, ❺ Token Distribution, ❻ Liquidity Removement, and ❼ Subsequent Actions.**

(3) *Token Deployment.* The token creator creates a new ERC-20 token and mints an initial supply of created tokens.

(4) *Liquidity Supplement.* The token creator often uses Uniswap V2: Factory Contract or Uniswap V3: Positions NFT to establish a liquidity pool by supplying both ETH and minted tokens.

(5) *Token Distribution.* The intermediate accounts in Step (2) can in turn swap their ETH for the newly minted token, as can opportunistic buyers swayed by speculative factors such as token branding or artificially inflated prices on AMM. The token creator can also transfer tokens to intermediate addresses.

(6) *Liquidity Removement.* The largest token holder (usually the creator) eventually withdraws all or most of the liquidity, rendering the token effectively untradeable. This action aggregates assets of other holders, including those of legitimate investors, into the token creator's account, completing a typical rug pull.

(7) *Subsequent Actions.* The token creator can then (a) cash out to fiat via CEX, (b) cycle the proceeds back into TC for further obfuscation, or (c) transfer the gains to another token creator account to repeat the scheme from Step (2) to Step (6).

Notably, this workflow is not limited to executing rug pull scams; it can also function as an obfuscation layer within broader crypto money laundering schemes. In Step (5), if no legitimate external participants engage in token purchases, assets originating from multiple intermediate accounts can be funneled into the address that ultimately removes most or all liquidity in Step (6). This maneuver aggregates value into a single destination, effectively masking the provenance of funds through the use of liquidity pools. To uncover the fund flow, investigators must identify the relevant liquidity pools, analyze token holder distributions, and determine which address accumulates the majority of the withdrawn liquidity for each created token. This additional layer of indirection significantly complicates transaction tracing and undermines traditional detection or censorship mechanisms.

**Crafted Tokens for Address Poisoning Scams.** Another misuse of crafted tokens involves address poisoning scams [18], one kind of phishing attacks based on the address similarity. Figure 11 provides an overview of this attack flow.

(1) *Initial TC Withdrawals.* The scammer begins by withdrawing ETH from TC, concealing the source of funds.

(2) *Fake Token Deployment.* Leveraging Ethereum's permissionless token-creation framework, the attacker deploys a fake ERC-20 token configured to mimic well-known assets such as native ETH, USDT, or USDC. By duplicating names and symbols, the attacker capitalizes on user familiarity and brand recognition. Notably, multiple scammers can share the same counterfeit token contract, thereby reducing overhead of broader phishing.

(3) *Batch Contract Deployment.* The scammer creates a specialized batch contract to streamline the distribution of phishing tokens. This contract can broadcast fraudulent token transfers in bulk, significantly reducing the gas costs per individual victim.

(4) *Blockchain Monitoring.* The scammer continuously monitors Ethereum transactions to identify promising targets (e.g., the address engaging with large-scale legitimate token trading). The scammer generate huge amount of addresses and select phishing addresses that closely resemble addresses (with the same hash prefix and suffix) in the victim's transaction history, aiming to induce confusion and unintended errors.

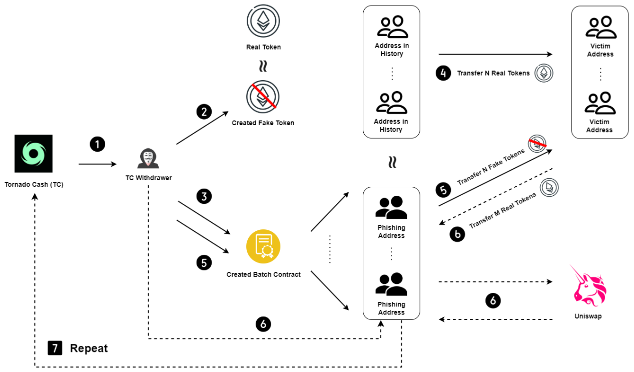

**Figure 11: Crafted Tokens for Address Poisoning Scams. The solid lines represent the preparation phase, and the dashed lines denote the process after the scams are successful. The workflow includes following steps: ❶ Initial TC Withdrawals, ❷ Fake Token Deployment, ❸ Batch Contract Deployment, ❹ Blockchain Monitoring, ❺ Address Poisoning, ❻ Profit Movement, and ❼ Subsequent Actions.**

(5) *Address Poisoning.* The fake token contract can deliberately exclude standard balance check logic, for instance, it can emit a `transferFrom` event listing the victim as the sender, even if the victim holds no balance of the counterfeit token. Since wallets and block explorers typically display the most recent transaction at the top of the history, such fabricated transfers can appear above legitimate ones. When combined with visually similar account addresses or token impersonation, this tactic can cause unsuspecting users to mistakenly send genuine assets to wrong account. Furthermore, distributing fake tokens via batch contracts allows scammers to bundle multiple deceptive transfers into a single transaction. This not only obfuscates the activity but also reduces gas costs, increases reachability, and minimizes detection risk by avoiding abnormal patterns.

(6) *Profit Movement.* If phishing addresses receive the asset from victims, the scammer sends a small amount of ETH to these addresses as transaction fees to fund the movement of profits. For example, swapping real tokens to ETH or other reputable tokens via DEX like Uniswap or 1inch.

(7) *Subsequent Actions.* Addresses controlled by scammers can then (a) cash out to fiat via CEX, (b) cycle the proceeds back into TC for further obfuscation, or (c) use profits to repeat the scamming scheme from Step (2) to Step (6).

# E MORE ANALYSES OF SERVICE USAGE

## E.1 Privacy-Enhancing Tools

Multiple privacy tools have emerged within the blockchain ecosystem, each employing distinct techniques to break the linkability between transactions. An advanced strategy observed in privacy-focused activities involves the sequential use of multiple privacy protocols, either at different stages of the transaction lifecycle or across different blockchains.

**Reuse of Tornado Cash.** TC itself also serves as a destination for assets previously withdrawn from its own pools. Our analysis identifies two prevalent patterns of reuse: *(i) Self-Loop*, where users withdraw funds from TC and redeposit nearly identical amounts back into TC, sometimes routing these assets through one or more intermediate addresses; and *(ii) Mix-up*, where withdrawn assets from TC are combined with external funds, thereby reducing the overall impurity score. In total, we detect 54,249.31 ETH involved in such reuse cycles, resulting in an impurity score $\varphi \approx 65.45\%$. Importantly, rapid increases in deposit volume that coincide with a sudden decrease in impurity scores may correlate with security incidents. Specifically, attackers initially seed an address with minor deposits from TC and later use the same channel to launder significant amounts of stolen crypto assets back into TC. This pattern aligns closely with 29 cases documented in Section 5.2.2.

**Private Proofs of Innocence in Railgun.** Railgun [33] is an Ethereum-based privacy solution that features a mechanism known as *Private Proofs of Innocence*. Deposits into newly created Railgun shielding tokens must wait for one hour to successfully pass an innocence proof before performing any interaction beyond an immediate refund to the originating address. If this proof fails, the funds are automatically returned to their source.

We observe the evolving adoption of this mechanism since its activation in November 2023 [31]. Interestingly, the first detected TC-related refund occurred much later, in June 2024, involving account 0x80Df...B1b0 at Block 20178593. Prior to this event, we identify transfers totaling 15,780.31 ETH, with impurity score $\varphi \approx 99.35\%$, directly from TC into Railgun that did not trigger innocence-proof mechanisms. This finding indicates that Railgun initially allows direct inflows from TC without imposing additional restrictions. Following this specific incident, the Railgun protocol begins to reject funds derived from TC. Nonetheless, there are over 2,320.55 ETH deposited into Railgun after the firs refund, but among them only around 506.75 ETH (21.84%) are refunded. This indicates that this mechanism is not effective and users can still successfully circumvent this restriction.

**Other Privacy-Preserving Tools.** Umbra [19] leverages stealth addresses to conceal recipient identities. Our analysis identifies 6,286.13 ETH transferred from TC into Umbra, carrying a notable impurity score $\varphi \approx 93.07\%$, underscoring its steady adoption. In contrast, Aztec Connect, previously a prominent Ethereum-based privacy solution with inflows of 2,244.93 ETH at impurity score $\varphi \approx 95.71\%$, ceased operations on March 31, 2023 [26], consequently diminishing its latest relevance. Similarly, another deprecated tool is the Secret Network: Bridge, which received 681.16 ETH with impurity score $\varphi \approx 98.71\%$. Its successor, Secret Tunnel powered by Axelar [35], continues providing user privacy within Secret Network, keeping on-chain transactions and balances fully confidential. Additionally, Nocturne [30] has emerged as a new privacy protocol on Ethereum. Although its adoption remains limited, only one TC withdrawer 0xA372...A19D appears in our dataset, its appearance indicates that newly developed privacy tools keep attracting user interests. Outside Ethereum, CoinJoin [22] remains the dominant privacy-enhancing technique for Bitcoin transactions. We frequently observe cases where funds originating from TC are transferred from Ethereum to Bitcoin via intermediaries like THORChain and SWFT Swap, subsequently funneled through CoinJoin transactions for additional obfuscation.

## E.2 Miscellaneous

Beyond the previously discussed well-known methods, several additional mechanisms also facilitate the broader circulation of cryptocurrency assets. In this section, we explore how these mechanisms can be leveraged by TC withdrawers.

**ETH Staking.** Following Ethereum's transition to PoS, users can stake amounts of 32 ETH to obtain rewards. Although ETH staking typically implies a long-term commitment, certain actors may leverage staking services, particularly liquid staking services that do not require minimum staking amount, to obscure the origin of assets under the appearance of legitimate staking activities. Once ETH is staked, it becomes significantly more difficult to accurately trace the origins of subsequent staking reward distributions. Effective tracking of these funds necessitates long-term monitoring of validator addresses and the continuous mapping of reward flows. Additionally, regulatory frameworks and compliance measures related to staking and associated rewards are currently less developed. These vulnerabilities are especially pronounced if staking services or pool operators fail to thoroughly scrutinize participant addresses. According to our database, TC-related funds account for 86.10% of the 26,419.12 ETH staked via Lido stETH, and 91.59% of the 16,960.00 ETH staked using the Beacon Deposit Contract.

**Multi-Sending.** Multi-sending contracts, also known as batch distribution or airdrop services, allow users to distribute funds to multiple addresses within a single transaction. By reducing transaction fees compared to operating transfers in separate transactions, multi-sending services become attractive not only for legitimate promotional activities but also for distributing the stolen assets and supporting address poisoning scams (e.g., dust-value token transfers, zero-value token transfers, and fake token transfers [18]). Malicious actors utilizing these tools can fragment assets into numerous transactions with smaller transfer amount, creating a complex transaction graph that complicates investigating efforts. In addition, they can deploy their own multi-sending smart contracts and then destroy them immediately after a single use, thus further hindering effective tracing and analysis. Based on our database, two prominent multi-sending services, Disperse.app and CoinTool: MultiSender, collectively processed 8,288.66 ETH, of which 77.57% are identified as TC-related funds.

**Lending.** Users can deposit TC-derived assets as collateral in decentralized lending platforms such as Aave [2] and Compound [10] to borrow other tokens. Provided they maintain sufficient collateral ratios, these actors can gradually shift borrowed assets into new addresses without immediate repayment or forced liquidation. Alternatively, actors may repay borrowed assets after a period of time, reclaiming their original deposits and thereby creating an additional layer of obfuscation. They may even simply maintain the collateral position over extended periods to accrue interest. Aave's front-end interface employs monitoring services by TRM Labs to restrict interactions involving addresses linked to TC activities, but malicious actors can circumvent these restrictions by directly interacting with the lending platform's underlying on-chain smart contracts. Based on our dataset, the combined volume of ETH involved in Aave and Compound lending platforms amounts to 28,393.55 ETH, exhibiting an impurity score $\varphi \approx 95.66\%$.

**NFT Trading.** The traditional art market has long been considered susceptible to misuse due to the subjective valuation of artworks. Similarly, NFT pricing also carries an inherently subjective valuation, making sudden large price increases less likely to raise suspicion compared to fungible tokens. Due to blockchain pseudonymity, distinguishing whether a seller and buyer are controlled by the same entity becomes particularly challenging. Malicious actors may exploit this by minting NFTs or purchasing existing NFTs from marketplaces, subsequently transferring them repeatedly between self-controlled addresses at artificially inflated prices. According to our dataset, 1,809.71 ETH associated with NFT tradings have been identified, with an impurity score $\varphi \approx 62.13\%$, as linked to TC withdrawers. We also highlight two NFTs that demonstrate strong indicators of wash trading activities: (1) NFT A was initially purchased for 0.0001 ETH in Transaction T1 by Address A1, after which the TC withdrawer A2 purchased NFT A from A1 at 20.9 ETH in Transaction T2; finally, A1 transferred the proceeds to FixedFloat; (2) NFT B similarly experienced a significant price jump from 0.0001 ETH to 9.925 ETH.

# F SUPPLEMENTARY EXPERIMENT RESULTS

This section presents additional experimental results and supporting evidence that complement our main analysis on the effectiveness of blockchain sanctions. Figure 12 illustrates the historical impurity metrics of the block producer rsync-builder. Figure 13 provides an example of the test-depositing pattern when users interact with services implementing censorship mechanisms.

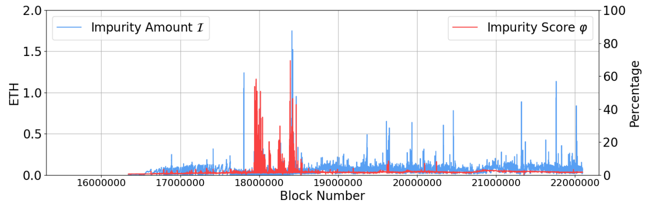

**Figure 12: Historical impurity amount and score of the block producer rsync-builder between $s_{OFAC}$ and $s_{END}$, in which its highest impurity score can reach $\varphi \approx 70\%$.**

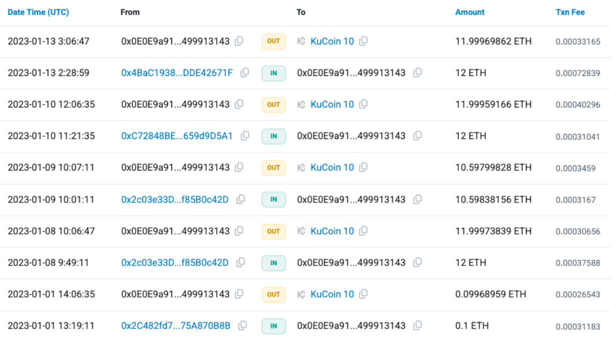

| Date Time (UTC) | From | | To | Amount | Txn Fee |
|---|---|---|---|---|---|
| 2023-01-13 3:06:47 | 0x0E0E9a91...499913143 | OUT | KuCoin 10 | 11.99969862 ETH | 0.00033165 |
| 2023-01-13 2:28:59 | 0x4BaC1938...DDE42671F | IN | 0x0E0E9a91...499913143 | 12 ETH | 0.00072839 |
| 2023-01-10 12:06:35 | 0x0E0E9a91...499913143 | OUT | KuCoin 10 | 11.99959166 ETH | 0.00040296 |
| 2023-01-10 11:21:35 | 0xC72848BE...659d9D5A1 | IN | 0x0E0E9a91...499913143 | 12 ETH | 0.00031041 |
| 2023-01-09 10:07:11 | 0x0E0E9a91...499913143 | OUT | KuCoin 10 | 10.59799828 ETH | 0.0003459 |
| 2023-01-09 10:01:11 | 0x2c03e33D...f85B0c42D | IN | 0x0E0E9a91...499913143 | 10.59838156 ETH | 0.0003167 |
| 2023-01-08 10:06:47 | 0x0E0E9a91...499913143 | OUT | KuCoin 10 | 11.99973839 ETH | 0.00030656 |
| 2023-01-08 9:49:11 | 0x2c03e33D...f85B0c42D | IN | 0x0E0E9a91...499913143 | 12 ETH | 0.00037588 |
| 2023-01-01 14:06:35 | 0x0E0E9a91...499913143 | OUT | KuCoin 10 | 0.09968959 ETH | 0.00026543 |
| 2023-01-01 13:19:11 | 0x2C482fd7...75A870B8B | IN | 0x0E0E9a91...499913143 | 0.1 ETH | 0.00031183 |

**Figure 13: One example of the test depositing pattern when users contentiously deposit into services with censorship mechanisms (i.e., KuCoin, a centralized exchange).**

Table 5 lists the top 20 impurity amount holders at the conclusion of our observation period, revealing the concentration points of sanctioned funds. Table 6 offers the active days and corresponding impurity volumes of CEX. Finally, Table 7 compares our algorithm's block-update times against typical block-production intervals.

**Table 5: Top 20 Impurity Amount Holders at $s_{END}$, in which 10 (50%) are CEX wallets and 7 (35%) are cross-chain bridges.**

| Class | Label | Impurity Amount $\mathcal{I}$ |
|---|---|---:|
| Staking | Beacon Deposit Contract | 382,383.25 ETH |
| DEX | Wrapped Ether | 53,826.27 ETH |
| Bridge | Arbitrum: Bridge | 42,006.84 ETH |
| Bridge | Base: Base Portal | 31,012.00 ETH |
| Bridge | Optimism: Portal | 17,288.26 ETH |
| CEX | Binance: Hot Wallet 20 | 11,419.47 ETH |
| CEX | Bitfinex 2 | 11,363.57 ETH |
| Bridge | ZKSync: Shared Bridge[†] | 8,853.93 ETH |
| CEX | Upbit 41 | 8,317.57 ETH |
| CEX | Ceffu: Custody Hot Wallet 2 | 5,062.12 ETH |
| CEX | Bitfinex: MultiSig 3 | 2,777.46 ETH |
| Bridge | Polygon (Matic): Ether Bridge | 2,630.76 ETH |
| CEX | Bithumb: Hot Wallet[‡] | 2,567.65 ETH |
| CEX | Gate.io 5 | 2,510.54 ETH |
| CEX | Bybit: Hot Wallet | 2,491.63 ETH |
| CEX | Crypto.com: Hot Wallet[‡] | 2,415.39 ETH |
| Bridge | Stargate: Pool Native | 2,337.40 ETH |
| Wallet | Gnosis Safe Proxy | 2,219.76 ETH |
| Bridge | Linea: L1 Message Service | 2,159.69 ETH |
| CEX | Kraken?[‡] | 1,897.21 ETH |
| | Accumulated Holding Impurity Amount | 600,815.50 ETH |
| | % of Post-Sanction Withdrawal Volume | 55.31 % |

[†] From the official ZKSync Docs website.
[‡] From the Arkham Intelligence platform
Other labels are from the Etherscan platform.

**Table 6: Active Span and Impurity Volume of CEX**

| CEX | Active Span (Days) | Impurity Volume $\mathcal{I}_v$ |
|---|---:|---:|
| Binance | 822 (85.89%) | 20,097.20 ETH (16.33%) |
| ChangeNOW | 802 (83.80%) | 3,942.41 ETH (03.20%) |
| FixedFloat | 702 (73.35%) | 25,450.88 ETH (20.68%) |
| eXch | 609 (63.64%) | 22,018.98 ETH (17.89%) |
| Coinbase | 584 (61.02%) | 960.88 ETH (00.78%) |
| KuCoin | 581 (60.71%) | 5,422.31 ETH (04.40%) |
| MEXC | 557 (58.20%) | 6,504.51 ETH (05.28%) |
| OKX | 500 (52.25%) | 15,420.37 ETH (12.53%) |
| Bybit | 430 (44.93%) | 3,064.73 ETH (02.49%) |
| SideShift | 286 (29.89%) | 1,452.07 ETH (01.18%) |
| HTX | 254 (26.54%) | 5,760.38 ETH (04.68%) |
| Kraken | 214 (22.36%) | 408.93 ETH (00.33%) |
| Gate.io | 203 (21.21%) | 4,007.67 ETH (03.26%) |
| Bitget | 115 (12.02%) | 546.41 ETH (00.44%) |
| SimpleSwap | 114 (11.91%) | 4,516.20 ETH (03.67%) |
| TradeOgre | 110 (11.49%) | 3,525.23 ETH (02.86%) |
| Total | 957 (100%) | 123,099.20 ETH (100%) |

**Table 7: Comparison with Ethereum and Other Platforms**

| Platform | Block Time[*] | Avg. TPS[*] |
|---|---:|---:|
| Ethereum | 12.06s | 13.98 tx/s |
| BNB | 3.00s | 62.72 tx/s |
| Tron | 3.00s | 98.01 tx/s |
| Arbitrum | 0.25s | 23.81 tx/s |
| Base | 2.00s | 83.89 tx/s |
| Optimism | 2.00s | 11.71 tx/s |
| Polygon | 2.14s | 36.96 tx/s |
| *Impurity Algorithm* | *0.07s* | *1500 tx/s* |

[*] From the Chainspect Platform in 30 days before April 10, 2025.

## G MACHINE SPECIFICATIONS

Our evaluation platform is powered by an AMD Ryzen 9 7900X processor (12 cores/24 threads) with a 4.7GHz base frequency and 5.6GHz boost clock; 64GB (2x32GB) DDR5-6000 CL36 DIMM memory in dual-channel configuration; and a WD_BLACK SN850X 4TB NVMe SSD with sequential read speeds up to 7,300MB/s and write speeds up to 6,600MB/s. The system runs Ubuntu 22.04.4 LTS with Linux kernel 6.8.0-45-generic. Software environment includes Rust compiler v1.83.0, Reth Ethereum execution client v1.1.3, and Lighthouse Ethereum consensus client v5.3.0.